Main species and chemical pathways in cold atmospheric-pressure Ar+H_2O plasmas

Dingxin Liu[1], Bowen Sun[1], Felipe Iza[2], Dehui Xu[1], Xiaohua Wang[1*], Mingzhe Rong[1] and Michael G Kong[1,3,4]

[1]State Key Laboratory of Electrical Insulation and Power Equipment, Centre for Plasma Biomedicine, Xi'an Jiaotong University, 710049, P. R. China
[2]School of Mechanical, Electrical and Manufacturing Engineering, Loughborough University, LE11 3TU, UK
[3]Frank Reidy Center for Bioelectrics, Old Dominion University, Norfolk, Virginia 23508, USA
[4]Department of Electrical and Computer Engineering, Old Dominion University, Norfolk, Virginia 23529, USA

Email: xhw@mail.xjtu.edu.cn

Abstract

Cold atmospheric-pressure plasmas in Ar+H_2O gas mixtures are a promising alternative to He+H_2O plasmas as both can produce reactive oxygen species of relevance for many applications and argon is cheaper than helium. Although He+H_2O plasmas have been subject of multiple experimental and computational studies, Ar+H_2O plasmas have received less attention. In this work we investigate the composition and chemical pathways in Ar+H_2O plasmas by means of a global model that incorporates 57 species and 1228 chemical reactions. Water vapor concentrations from 1 ppm to saturation (32000 ppm) are considered in the study and abrupt transitions in power dissipation channels, species densities and chemical pathways are found when the water concentration increases from 100 to 1000 ppm. In this region the plasma transitions from an electropositive discharge in which most power is coupled to electrons into an electronegative one in which most power is coupled to ions. While increasing electronegativity is also observed in He+H_2O plasmas, in Ar+H_2O plasmas the transition is more abrupt because Penning processes do not contribute to gas ionization and the changes in the electron energy distribution function and mean electron energy caused by the increasing water concentration result in electron-neutral excitation and ionization rates changing by many orders of magnitude in a relatively small range of water concentrations. Insights into the main chemical species and pathways governing the production and loss of electrons, O, OH, OH(A) and H_2O_2 are provided as part of the study.

1. Introduction:

Cold atmospheric-pressure plasmas (CAPs) have shown promise in a wide-range of applications including environmental protection[1-3], surface modification[4-6] and biomedicine[7-9]. Although the detailed underlying mechanisms governing these plasmas remain not fully understood, it is widely accepted that plasma-generated reactive oxygen species (ROS), such as OH, O_2^- and O, play a key role in most applications[10,11].

Water vapor is an efficient precursor for the production of these ROS in CAPs and therefore it is sometimes introduced in the feed gas[12-14]. For example, a water vapor concentration of ~1% is found to be optimum for the production efficacy of H_2O_2 in a radio frequency capacitively coupled He+H_2O plasma[15]. Being able to tune and optimize the yield of ROS for different CAP applications is one of the reasons behind the growing research in water-containing plasmas in recent years[16-18]. Another reason is that water vapor is present in most CAP systems even if this is not actively introduced in the feed gas and therefore understanding the impact that the presence of water has on the performance of a CAP system is vital. For example, even high-purity industrial helium gas has water vapor in concentrations higher than 1 part per million (ppm)[19]. CAPs in open air contain typically water vapor in concentrations of ~1%[20] due to the mixing of feed gases with humidity in the environment and this concentration increases to saturation (~3%) in CAPs generated inside or in contact with liquid water[21]. Considering that water in concentrations of just parts per million can influence the plasma composition[22], water vapor in concentrations of a few percent are bound to be important.

The chemistry in water-containing CAPs is complex and quantitative studies have proved to be very challenging. Dozens to hundreds of reactive species are normally generated in these CAPs but only a few of them can be readily measured with current diagnostic techniques[10]. Complementing experimental measurements, plasma modeling can provide additional insights into the physic-chemical mechanisms governing CAPs. Fluid models are most commonly used for the study of CAPs but for water-containing plasmas the computational load is so heavy that only a few fluid models with simplified chemistry sets have been reported in the literature[23-25].

In the past few years, global models have also been used to study CAPs[22,26-28]. These global models require less computational resources than fluid models due to the elimination of space dependences and hence they are well-suited for the study of complex plasma chemistry sets as those generated in water containing CAPs. Global models have successfully been used to identify key plasma species and to elucidate underlying chemical pathways in CAPS with complex plasma chemistry such as He+O_2+H_2O[29] and Ar+humid air [30].

Most studies of water containing CAPs use helium as a background gas. Helium has a good thermal conductivity and aids in keeping the gas temperature in the plasma low. However, helium is expensive and for many applications it would be beneficial to find lower-cost alternative carrier gases. That motivates our interest in Ar+H_2O CAPs and their chemistry.

In this paper, the chemistry of Ar+H_2O CAPs is studied for water vapor concentrations spanning from 1 ppm to saturation (32000 ppm)[31] using a global model that incorporates 57 species and 1228 volume reactions. Emission spectroscopy is used to measure the relative densities of OH(A) and experimental results are compared with computational predictions to benchmark simulation results.

The paper is structured as follows. The global model and the experimental setup are described in section 2. Simulation results are presented in section 3, where density trends, plasma characteristics and generation/loss mechanisms of selected ROS are discussed as a function of the water vapor concentration in the feed gas. Finally, concluding remarks are given in section 4.

2. Global model and its validation

A global model of an Ar+H_2O CAP sustained between two parallel-plate circular electrodes of radius R=1 cm is used in this study (see Figure 1). A sheet of quartz glass (thickness 0.1 cm) is placed on the bottom electrode and the gas gap between the glass sheet and the top electrode is 0.1 cm. The discharge is excited by an RF source (f=13.56 MHz) that delivers an average power density of 10 W/cm^3. The gas temperature is assumed to be 300 K, and the gas flow rate is set to be 0.1 SLM (Standard Liters per Minute). This configuration reflects the experimental setup used for the experiments discussed below. The water fraction in the Ar+H_2O feedstock gas is varied from 1 ppm to 32000 ppm (saturation).

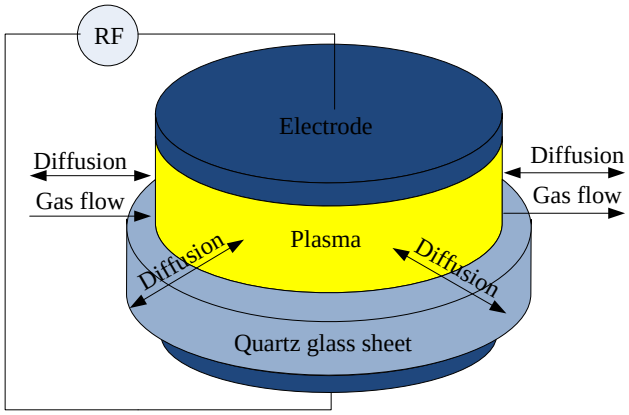

Figure 1. Schematic diagram of the model

57 species are considered in the global model and these are listed in Table 1. Based on prior studies of other water containing CAPs (He+H_2O[22,32], He+ humid air[28], Ar+

humid air[30]), hydrated ions are expected to be abundant and these have been included in the model. A total of 1228 volume reactions have been identified following an extensive literature review and their rate coefficients are listed in the Appendix. Most of the rate coefficients are taken from the literature, some have been calculated based on cross section data and when data was not available, rates have been estimated according to the recommendations in [33,108]. The Boltzmann solver BOLSIG+[34] was used to calculate the rate coefficients of electron-neutral reactions using cross section data from the literature.

Table 1. Species considered in this model

Type	Species
Hydrated cations	H_3O^+, $H_2O_2^+$, $H_4O_2^+$, $H_4O_4^+$, $H_2O_3^+$, $H_5O_2^+$, $H_7O_3^+$, $H_9O_4^+$, $H_{11}O_5^+$, $H_{13}O_6^+$, $H_{15}O_7^+$
Other cations	O^+, O_2^+, H^+, H_2^+, H_3^+, OH^+, HO_2^+, H_2O^+, Ar^+, Ar_2^+, ArH^+, O_4^+, O_6^+
Hydrated anions	$H_2O_2^-$, $H_3O_2^-$, $H_5O_3^-$, $H_2O_3^-$, $H_2O_4^-$, $H_4O_4^-$, $H_6O_5^-$, $H_4O_5^-$
Other anions	e^-, H^-, O^-, O_2^-, OH^-, O_3^-, O_4^-
Metastables	$Ar(^4S)$, $Ar(^4P)$, Ar_2^*, $O(^1D)$, $O(^1S)$, $O_2(a)$, $O_2(b)$, OH(A)
Grounded neutrals	Ar, H_2O, H, O, H_2, O_2, O_3, OH, HO_2, H_2O_2

The plasma chemistry is affected not only by volume reactions but also by wall reactions at the solid plates (the metal electrode and the quartz glass sheet) and sidewise diffusion and advection through the interface between the plasma and the surrounding gas (see Figure 1). Therefore, the particle balance equation for each plasma species is given by[35]:

$$\frac{dn_k}{dt} = G_k^V + \frac{S_1}{V}\left(\sum_{i=1,i\neq k}^{N} \alpha_{i,k}\Gamma_{1i} - \beta_k\Gamma_{1k}\right) - \frac{S_2}{V}\Gamma_{2k} - \frac{F}{V}n_k \quad (1)$$

where n_k is the number density of species k, G_k^V the net generation/loss rate of species k due to volume reactions in the plasma, N the total number of species, S_1 the total area of the solid plates, S_2 the "sidewall" area of the plasma-gas interface, V the plasma volume, Γ_{1k} the flux of species k to the solid plates, Γ_{2k} the flux of species k to the sides out of the plasma, and F the gas flow rate.

The second term on the right-hand side of equation 1 represents the particle gain/loss due to surface reactions, in which β_k is the surface reaction probability of species k, and $\alpha_{i,k}$ a parameter between zero and one that relates to the generation probability of species k due to surface reactions of species i. All cations are assumed to neutralize when reaching the walls and therefore β_k=1 for positively charged ions. On the other hand, anions are assumed to be confined by the ambipolar field and therefore $\beta_k\Gamma_{1k}$=0[36,37]. For neutral species, the value of β_k varies between zero and one depending on the species[22].To account for the collisionality of the sheaths, the flux of positive ions is calculated using the following expression[35]

$$\Gamma_{1k} = \frac{0.6 n_k u_B}{\sqrt{1+\frac{\pi\lambda_{Ds}}{2\lambda_{ion}}}} \quad (2)$$

where u_B represents the Bohm velocity, λ_{Ds} the Debye length in the plasma sheath, λ_{ion} the mean free path of positive ions. The pre-factor 0.6 in equation 2 accounts for the drop in plasma density that occurs from the center of the plasma to the sheath edge, while the denominator in equation 2 accounts for the drop in ion velocity at the collisional sheath edge compared to the Bohm velocity in collisionless low-pressure plasmas[22,38]. The drop value of ion velocity is ~40 from our calculation. All the positive ions are assumed to be neutralized on the solid plates. Finally, the electron flux is set to balance the total flux of positive ions, maintaining quasi-neutrality in the bulk plasma. No secondary electron emissions have been considered in the model, and hence the difference between the metal electrode and the quartz glass sheet is neglected.

The third term on the right-hand side of equation 1 represents the particle gain/loss due to sidewise diffusion. The sidewise gain/loss is estimated for the neutral species as reported in [36]. The feedstock gas consists of Ar and water vapor. Since only a small proportion of the argon gas is transformed into other species (such as argon metastables), the background argon concentration is assumed to be uniform and constant. However, this is not the case for water vapor as a large portion of the water molecules are dissociated and/or ionized in the plasma. So, the water vapor diffuses from the surrounding gas into the plasma region where it is consumed, and thereforeΓ_{2k} for H_2O is given by[36]

$$\Gamma_{2k} = \frac{2D_{H_2O}}{R}\left(1-\frac{n_{H_2O,ext}^2}{n_{H_2O}^2}\right)n_{H_2O} \quad (3)$$

where $n_{H_2O,ext}$ represents the number density of water vapor in the surrounding (feed) gas, n_{H_2O} the average density of water vapor in the plasma region, D_{H2O} the diffusion coefficient of water molecules which is calculated following the approach described in reference [39].

Different to the feedstock gas, other plasma species are generated in the plasma and then diffuse outwards. For long-lived species such as H_2, O_2, O_3, HO_2 and H_2O_2, Γ_{2k} is given by[36]

$$\Gamma_{2k} = \frac{2D_k}{R}\left(\frac{n_{H_2O,ext}}{n_{H_2O}}+1\right)n_k \quad (4)$$

On the other hand, for short-lived reactive species such as H and O, Γ_{2k} is given by[36]

$$\Gamma_{2k} = Z_k D_k \frac{n_{H_2O,ext}}{n_{H_2O}} n_k \quad (5)$$

where the coefficient Z_k is a function of the thermal velocity,

the gap width and the surface reaction probability of species *k*. The sidewise fluxes estimated by formulae (3)-(5) take into account the radial inhomogeneity of the plasma and their values are typically 1~3 orders of magnitude lower than the thermal flux ($0.25n_k v_{th}$). For charged species, $\Gamma_{2k}$is assumed zero as their flux will be controlled primarily by drift caused by electric fields. The last term on the right-hand side of equation 1 represents the particle gain/loss due to gas flow.

Reaction rates needed to determine the generation/loss of species in the plasma (G_k^V) depend on the mean electron energy, which is obtained by solving the electron power balance equation as follows[40]:

$$\frac{d}{dt}\left(\frac{3}{2}n_e T_e\right) = \xi\left(\frac{P_{in}}{eV} - \frac{S_1}{V}\left(\varepsilon_e \Gamma_e + \sum_{j=1}^{N_p}\varepsilon_p \Gamma_{1j}\right)\right) - \sum_{i=1}^{N_r}\varepsilon_i R_i \quad (6)$$

where n_e represents the electron density, T_e the mean electron temperature, ξ the ratio of power coupled to electrons, e the elementary charge, P_{in} the input power, N_r the number of electron impact reactions, ε_i and R_i the electron energy loss due to the *i*th electron impact reaction (including electron-neutral momentum transfer collision) and the corresponding reaction rate, ε_e and ε_p the energy lost per electron and ion escaping the plasma across the sheaths. The electron energy is assumed to be ε=1.5$n_e T_e$ based on the Maxwellian assumption. P_{in} is set constant to be 10 W/cm^3 (neglecting its periodic variation) for greatly reducing the computational load, and this simplification is acceptable for a RF discharge as predicted previously[40].

In electropositive plasmas it is safe to assume that current in the bulk plasma is carried by electrons because the electron and ion densities are comparable and the electron mobility is ~100 times larger than that of the ions[41].However, H_2O-containing CAPs can become electronegative and the concentration of electrons in the bulk plasma can be much lower than that of ions. As a result, significant amount of current can be carried by ions, affecting the way the input power is dissipated in the discharge. The fraction of the current carried by electrons can be estimated by[36,40,42]:

$$\xi = \frac{\mu_e n_e}{\mu_e n_e + \sum_k \mu_{i,k} n_{i,k}} \quad (7)$$

where μ_e is the electron mobility, $\mu_{i,k}$ the mobility of ionic species *k*, and $n_{i,k}$ the density of ionic species *k*.

Equation (1) and (6) are integrated using a custom MATLAB code that makes use of the built-in stiff ordinary differential equations solver *ode23s* to solve for the evolution of the electron temperature and species densities[29,35,40]. A plasma-on time of more than one second is needed to reach a steady state solution, for which the density of each plasma species changes less than 1% during 0.1 s.

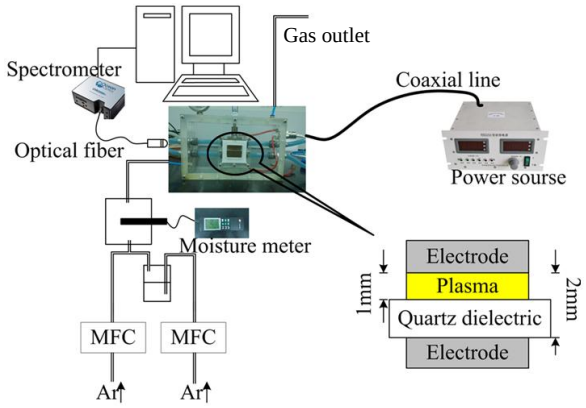

Figure 2. Experimental setup

In order to validate the simulation results, Ar+H_2O plasmas were generated by an RF power supply (*f*=13.56 MHz) and the plasma-generated OH(A) was detected by emission spectroscopy. The experimental set up is depicted in Figure 2. The input power was obtained by subtracting the reflection power from the incident power of the RF power source, which corresponds to the same power density of 10 W/cm^3 as the global model. It should be noted that the input power is from the source to the electrodes, not exactly absorbed by the plasma (a small portion of the power would be consumed by heating the electrodes). Water content in the feed gas was controlled by combining the flow of two argon (5N) channels, one of which was bubbled through a deionized water container. The flow in each channel was controlled by a mass flow controller (Aalborg, DFC) and the combined gas flow rate was kept constant at 2 SLM. Taking into account the geometry of the experimental setup, the gas flow rate through the plasma region was estimated to be 0.1 SLM. The water fraction in the mixed gas was measured by a moisture meter (Testo 654) and this was found to be proportional to the gas flow rate in the branch that passes through the water container. OH(A) produced in the plasma was measured using an Ocean Optics, Maya2000Pro spectrometer. The intensity of the emission spectral line at 308.9nm is known to be proportional to the density of OH(A).

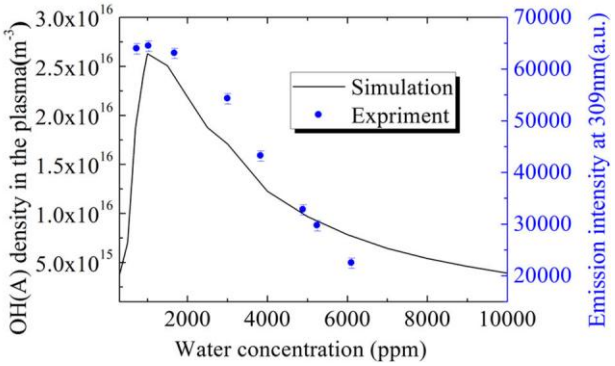

Figure 3. Comparison between the OH(A) densities in numerical and experimental studies

Comparison between the numerical and experimental results is shown in Figure 3. Experiments were only conducted for water vapor concentrations that ranged from 737 ppm to 6108 ppm. It was found difficult to control the water concentration below 737 ppm in a repeatable way due to limitations in the available equipment and the influence of residual water on the inner walls of the experimental setup. On the other hand, water concentrations above 6108 ppm resulted in unstable plasmas, i.e. the plasma column is contracted and filaments can be observed.

As shown in Figure 3, the calculated density of OH(A) peaks at a water vapor concentration of [H_2O]~1000 ppm, in agreement with the spectral line intensity at 308.9 nm. This qualitative agreement between simulation and experimental results provide some reassurance that despite its intrinsic limitations, the computational model can actually predict experimental trends and provide insights into the underlying discharge mechanisms.

3. Results and discussions

In order to quantify the amounts of reactive species produced in Ar+H_2O CAPs as well as to elucidate the chemical kinetics as a function of the water vapor concentration, simulations have been run for the following water concentrations: 1, 3, 10, 30, 100, 300, 1000, 3000, 10000 and 32000 ppm. The latter corresponds to the saturation concentration of water vapor and given its special significance the simulation results at that concentration are marked with a "star" symbol in the figures below. For many applications of CAPs (e.g. treatment of biological samples) the treated sample is either humid or a liquid. As a result, in the plasma region adjacent to the sample the water concentration is high, reaching saturation at the gas-liquid interface[43,44,45]. While sustaining a uniform discharge in water saturated gas is experimentally challenging (e.g. in the current experimental setup, water concentrations above 6108ppm turn the discharge unstable), the actual water concentration in most CAPs is not homogeneous[46]: a region of relatively dry gas away from the sample enables stable operation of the plasma while near the sample the humidity can increase up to saturation levels. Since most of the reactive species in the plasma diffuse only a few to several hundred microns during their lifetime in the plasma[47 - 49],it is important to understand the plasma chemistry in saturated gas as this is likely to determine the plasma chemistry that is "felt" by the treated samples. Experimental measurements of species and chemical kinetics in the saturated gas interface are very challenging and computational studies can provide valuable insights.

A. Densities of reactive species as a function of water vapor concentration

The density of cations generated in Ar+H_2O CAPs as a function of the water concentration in the feed gas are shown in Figure 4. For clarity, the cations are divided into two groups: non-hydrated cations (Figure 4a) and hydrated cations (Figure 4b). The overall cation density as a function of water concentration is not monotonous (see figure 4), indicating the presence of two regimes. The total cation density first decreases with increasing water content and then increases, having a minimum at [H_2O]~1000 ppm. At low water concentrations ([H_2O]<1000 ppm) Ar_2^+ions are the most abundant ionic species whereas as water content increases above 1000 ppm, heavier hydrated ions such as $H_{11}O_5^+$, $H_{13}O_6^+$ and $H_{15}O_7^+$ dominate successively. Small water derived cations such as H_2O^+, HO_2^+, H_3O^+, and ArH^+ are produced in significant quantities only at water concentrations of 10-300 ppm and their contribution to the cation population decreases very rapidly at lower or higher water concentrations.

It is noted that except for Ar^+, which is actually produced in relatively small quantities, the concentration of cations experience a strong transition at a water concentration of ~500 ppm. This transition is driven by 1) the increasing concentration of heavy-hydrated ions and 2) the changes in electron-impact reaction rates as water concentration increases from 100 to 1000 ppm. These changes of reaction rates are a consequence of the changes in electron density, electron temperature as well as electron energy distribution function.

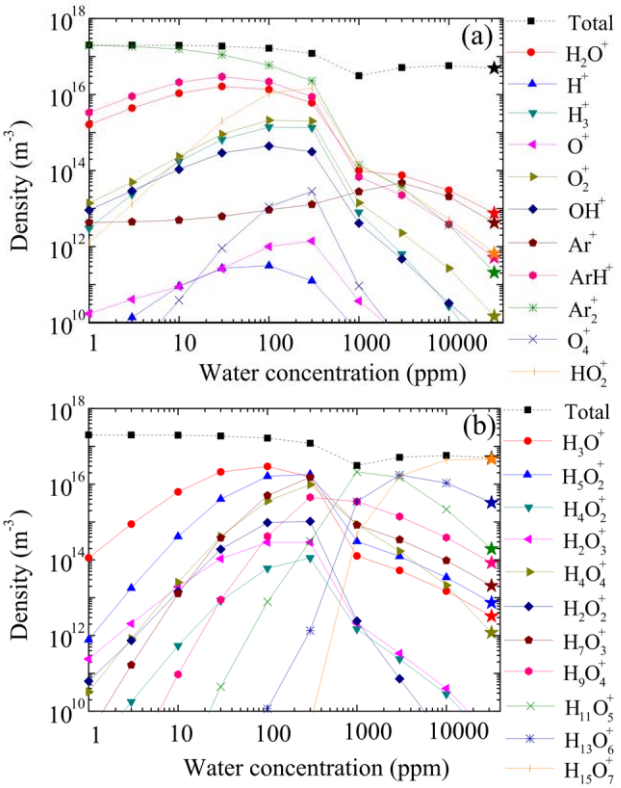

Figure 4. Densities of cations as a function of water vapor concentration: (a) Non-hydrated cations; and (b) hydrated cations.

Water vapor is an electronegative gas and hence anions are generated when water is introduced in the discharge (see

Figure 5). The total anion density increases from 5.0×10^{14} to 4.9×10^{16} $m^{-3}$when the water concentration increases from 1 ppm to 3000 ppm but it remains approximately constant for water concentrations above 3000 ppm. For water concentrations above ~1000 ppm the concentration of anions become comparable to that of cations, indicating that the plasma becomes strongly electronegative at high water concentrations. Similarly to the observation made for cations, heavier hydrated ions become increasingly abundant as the water concentration increases and a transition is observed as the water concentration increases from 100 to 1000 ppm. Biologically relevant species such as OH^-, O_2^- and $H_3O_2^-$are found to be produced in relatively large quantities, particularly at water concentrations of ~300 ppm.

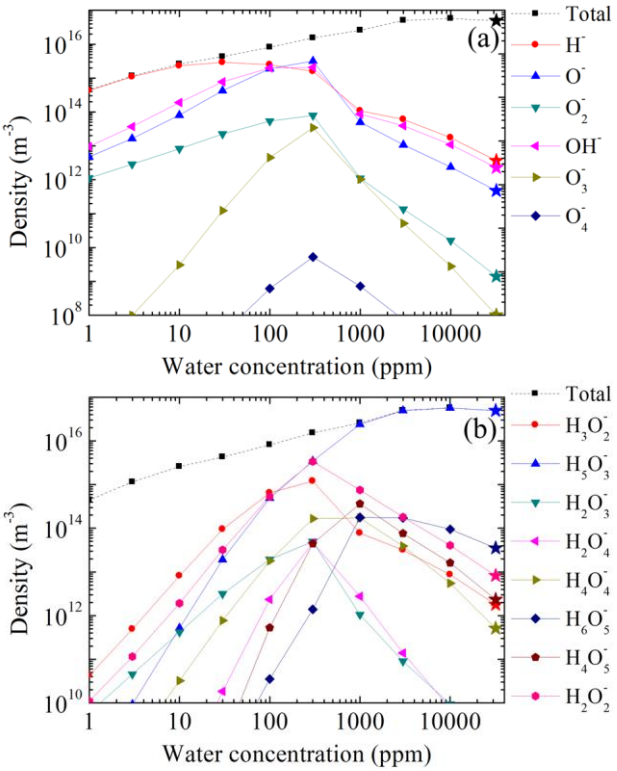

Figure 5. Densities of anions as a function of the water vapor concentration in the feed gas: (a) Non-hydrated anions; and (b) hydrated anions.

Figure 6 shows the dependence of the electron density, electron temperature and electronegativity on the water concentration in the feed gas. It can be seen that the electron density decreases from 2×10^{17} m^{-3} to 1×10^{14} m^{-3} while the electron temperature increases monotonously from 3.0 eV to 4.2 eV as the water vapor concentration increases from 1 ppm to saturation. The electronegativity, i.e. the ratio of anion concentration to electron concentration, increases rapidly at high water concentrations ([H_2O]>1000 ppm), reaching a value of ~470 at saturation.

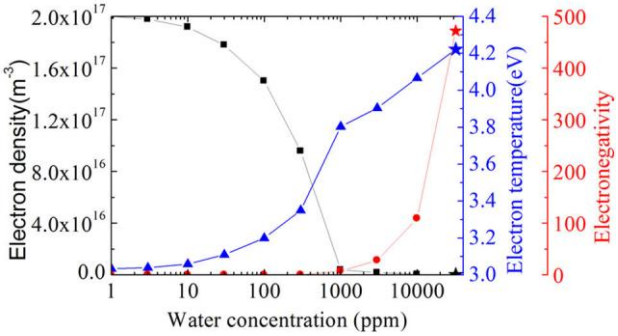

Figure 6. Electron density, electron temperature and electronegativity as a function of the water vapor concentration in the feed gas (Electron density; Electron temperature; Electronegativity)

In particular, the electron density decreases by more than one order of magnitude as the water concentration is increased from 100 to 1000 ppm. This decrease in electron density occurs at the same water concentrations at which rapid changes in ion densities were observed in figures 4 and 5 and reflects a rapid transition from an electron-positive into an electronegative plasma. The electron temperature is found to increase by ~0.6 eV in that transition region, as higher ionization is required to compensate for the increasing loss of electrons in attachment reactions.

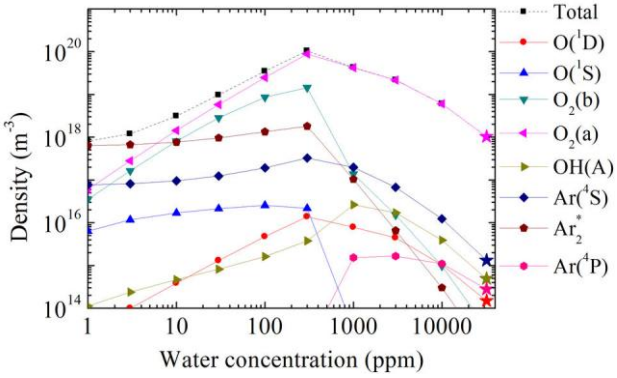

Figure 7. Density of excited neutral species as a function of the water vapor concentration in the feed gas.

The density of excited neutral species as a function of the water concentration in the feed gas is shown in Figure 7. The overall trend differs from that of ionic species (Figures 4 and 5). At first, the total density of excited neutral species is found to increase with increasing water concentration, reaching a maximum at [H_2O]~300 ppm. Above that water concentration, the density of neutral excited species decreases. This decrease is attributed not only to the fast decrease in electron density (Figure 6) but also to the quenching of excited species by water molecules [50,51]. Therefore, for the generation of excited neutral species, the optimal water concentration in the feed gas is ~300 ppm. The total density of excited neutral species is larger than that of the charged species (Figure 4and 5) by one to two

orders of magnitude across the whole range of water concentrations. At very low water content $Ar_2^*$is the most abundant excited species but O_2(a) becomes the dominant species for water concentrations above 10 ppm. The density trend of OH(A) is similar to that of O_2(a) but the magnitude is about three orders of magnitude lower and it peaks at slightly higher water concentration. According to this simulation results, the maximum density of OH(A)occurs at $[H_2O]$=1000 ppm, which agrees with experimental measurements reported in the literature using the 308.9 nm spectral line intensity (OH(A)→OH(X)+hν)[52,53].

The main ground state species generated in Ar+H_2O CAPs are H, O, H_2, O_2, OH, HO_2, H_2O_2 and O_3, and their concentration as a function of the water content in the feed gas is shown in Figure 8. The dot line represents the original water vapor density in the feed gas, and the red curve with circle symbols represents the water density in the active plasma. It is interesting to note that the water vapor concentration in the plasma is about 1 order of magnitude lower that in the feed gas when $[H_2O]\leq$300 ppm. This is because most water molecules are dissociated into H, O, OH by electron impact reactions in this regime. At high water concentration ($[H_2O]$>1000 ppm), a smaller fraction of the water is dissociated due to the increasing water content and the lower electron density (Figure 6).

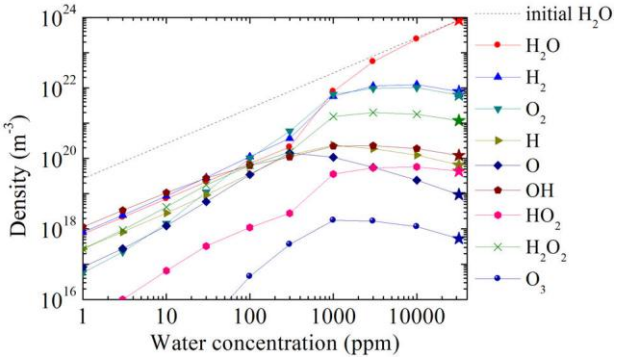

Figure 8. Density of ground neutral species as a function of the water vapor concentration in the feed gas

OH is the most abundant ground state neutral species when $[H_2O]$<30 ppm, and OH, H_2 and $O_2$are found to be more abundant than water molecules in the active plasma for water concentrations in the feed gas <1000 ppm. The density of O first increases and then decreases with increasing water vapor concentration and peaks at $[H_2O]$~300 ppm. The densities of other biologically relevant reactive species such as OH,HO_2 and H_2O_2alsoincrease with increasing water content reaching a maximum at $[H_2O]$~1000 ppm. This implies that maximum production of these reactive species can be achieved without compromising the plasma stability.

The density of OH is higher than that of its excited state OH(A) by more than three orders of magnitude and significantly their trend at water concentrations above 1000 ppm are quite different (see Figure 7 and 8). This implies that one should be careful when inferring OH production from OH(A) emission lines[54]. Experimental data using cavity ring down spectroscopy to measure OH radicals in an Ar+H_2O CAP has shown that OH density reaches a maximum value when $[H_2O]$~1.5%[16]. These experimental results agree with the simulation results presented in this paper. Also in agreement with experimental measurements is the observation that at high water concentration the density of $H_2$and O_2 (figure 8) is higher than that of H_2O_2 by more than one order of magnitude[55].

It is well-known that water quenches the production of ozone and for all the water concentrations investigated in this study the O_3 concentration is found to be <0.2ppm. This concentration is lower than the recommended limit (100 μg/m^3) of the WHO Air Quality Guidelines[56], suggesting that Ar+H_2O CAPs may be able to meet environmental requirements more readily than other dry O_2-rich CAPs, such as Ar+O_2or He+O_2plasmas.

B. Power dissipation

Figure 9 shows the main channels in which energy delivered the plasma is dissipated. When the water concentration in the feed gas is small (<300 ppm), the input power is mainly consumed in elastic collision (Momentum transfer collsion) between electrons and background gas molecules. Despite the small energy transfer in each elastic electron-neutral collision, the large collisionality encountered in atmospheric-pressure plasmas results in these collisions dominating the power balance. As the water concentration increases, so does the electron temperature (see Figure 6) and inelastic collisions become increasingly important. For water concentrations between 300 ppm and 3000 ppm, most power delivered to the plasma is dissipated in inelastic electron-neutral collisions. In these regime, the reactions consuming most power are:

$$e+Ar\rightarrow Ar(^4S)+e \quad (R73)$$

$$e+Ar\rightarrow Ar(^4P)+e \quad (R74)$$

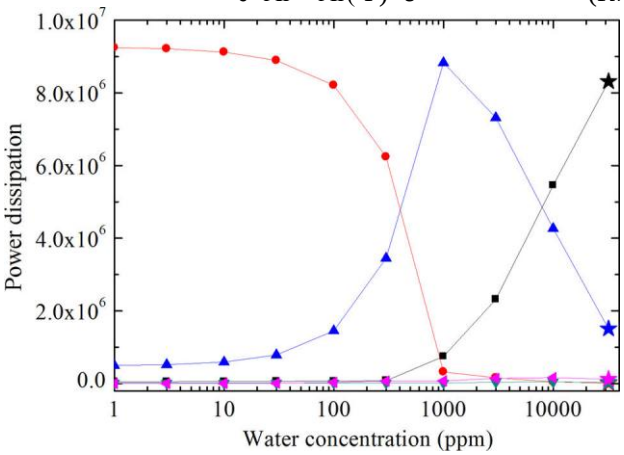

Figure 9. Power dissipations as a function of the water vapor concentration (—■—: Ion Joule heating —●—: Elastic collisions —▲—: Electron excitation —▼—: Ionization —◄—: Other inelastic collisions)

At water concentrations above 3000 ppm, the discharge is strongly electronegative and most power is coupled to ions instead of to electrons. As a result, at high water concentrations the main dissipation channel is ion Joule heating (See equation 7 and accompanying discussion).This would result in significant gas heating and as observed experimentally lead to instabilities in the discharge. In comparison, the power dissipation in other inelastic collisions (including vibrational excitation, ionization, etc.) is small.

As shown in Figure 9, the ratio of power dissipated in elastic collisions to the total input power drops sharply from 82% to 3% when the water concentration increases from 100 to 1000 ppm. At the same time, the ratio of power dissipated in inelastic collisions increases from 17% to 88%. Such rapid transitions are a reflection of significant changes in the discharge conditions. Similar transitions were observed in species densities (Figures 4 to 8) and chemical pathways (see discussion below). These changes are linked to a rapid increase in the rate coefficient of inelastic reactions as the electron temperature increases with increasing water content.

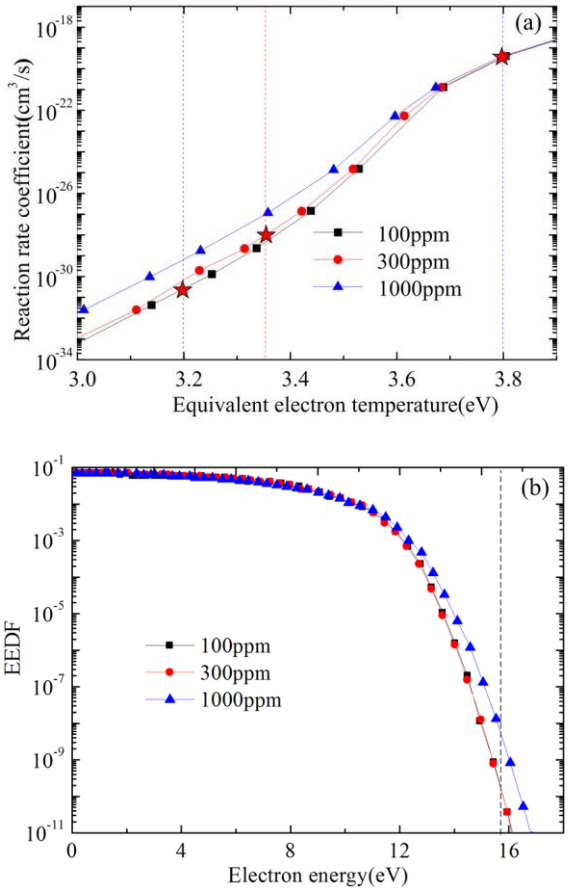

Figure 10. Variations of the reaction rate coefficient of e+Ar→Ar^++2e (a) and the electron energy distribution function (b) in Ar+H_2O CAPs with different water vapor concentrations. The star symbols in Figure 10(a) represent the reaction rates at the self-consistent equivalent electron temperatures (2/3 mean electron energy) according to the simulation results. All the EEDF curves in Figure 10(b) are at a given mean electron energy of 5.25 eV.

Taking the reaction e+Ar→Ar^++2e (R30) as an example, the rate coefficient increases by more than 12 orders of magnitude when the water vapor concentration increases from 100 to 1000 ppm, as represented by the star symbols in Figure 10(a). This increase occurs as a result of an increase in electron temperature (from 3.2 eV to 3.8 eV) and changes in the electron energy distribution function (EEDF). In order to describe the change of EEDF, we plot in Figure 10(b) the EEDFs for the water concentrations of 100, 300 and 1000 ppm at a given mean electron energy of 5.25 eV (equivalent to an electron temperature of 3.5 eV). It can be seen that the EEDF keeps similar for [H_2O]=100 and 300 ppm, but it changes significantly with the increasing water concentration from 300 to 1000 ppm. The change is especially in its high-energy portion of ε>15.76 eV (as indicated by a dash line in Figure 10(b)), in which the electrons are capable of ionizing argon molecules (R30). The EEDF is also obtained by the Boltzmann solver BOLSIG+, and its variation is mainly attributed to the changing nature of the background molecules as admixture of water vapor is introduced and products such as (H_2, O_2, H_2O_2, etc.) are generated.

C. Main physicochemical pathways of selected reactive species

From an application point of view, it is of interest to elucidate the production/loss mechanisms of some key species. In this section we discuss the generation and loss of electrons, O, OH(A), OH and H_2O_2.

The main pathways for the generation and loss of electrons as a function of the water content in the feed gas are shown in Figure 11. As observed in previous graphs, a clear transition occurs as the water concentration in the feed gas increases from 100 to 1000 ppm. At low water concentrations the discharge is sustained primarily by ionization of excited argon species (R32 and R31). This stepwise ionization accounts for 87% of the electron production. Reactions R32, R31 and R1140 are in decreasing order of significance the key reactions for electron production at low water concentration:

$e+Ar_2^* \rightarrow Ar_2^+ +2e$ (R32)

$e+Ar(^4S) \rightarrow Ar^+ +2e$ (R31)

$2Ar_2^* \rightarrow Ar_2^+ +2Ar+e$ (R1140)

As the water concentration increases above 300 ppm, electron-impact ionization of argon atoms (R30) and water molecules (R6) become the dominant electron production pathways, followed by collisional detachement (R1042 and R984):

$e+Ar \rightarrow Ar^+ +2e$ (R30)

$e+H_2O \rightarrow H_2O^+ +2e$ (R6)

$H_5O_3^- +H \rightarrow 3H_2O+e$ (R1042)

$H^- +O_2 \rightarrow HO_2+e$ (R984)

The shift in electron production pathways from R32 and R31to R30 and R6 is due to 1) the rapid increase in the reaction rate of reaction R30as the electron temperature increases (see Figure 10), and 2) the increased quenching of argon metastables by water molecules at high water concentrations (e.g. R1127: $Ar(^4S)+H_2O\rightarrow Ar+OH+H$).

Regarding the loss of electrons, at low water concentrations ($[H_2O]$<300 ppm) the electrode loss is the main loss process, with a small contribution of electron-ion recombination reactions (R126 and R117):

$$e+Ar_2^+\rightarrow 2Ar \quad (R126)$$

$$e+H_5O_2^+\rightarrow 2H_2O+H \quad (R117)$$

However, as the water concentration increases above 300 ppm, most electrons are lost in volume reactions in the plasma, in particular through dissociative attachment of water molecules:

$$e+H_2O\rightarrow H^-+OH \quad (R86)$$

$$e+H_2O\rightarrow O^-+H_2 \quad (R87)$$

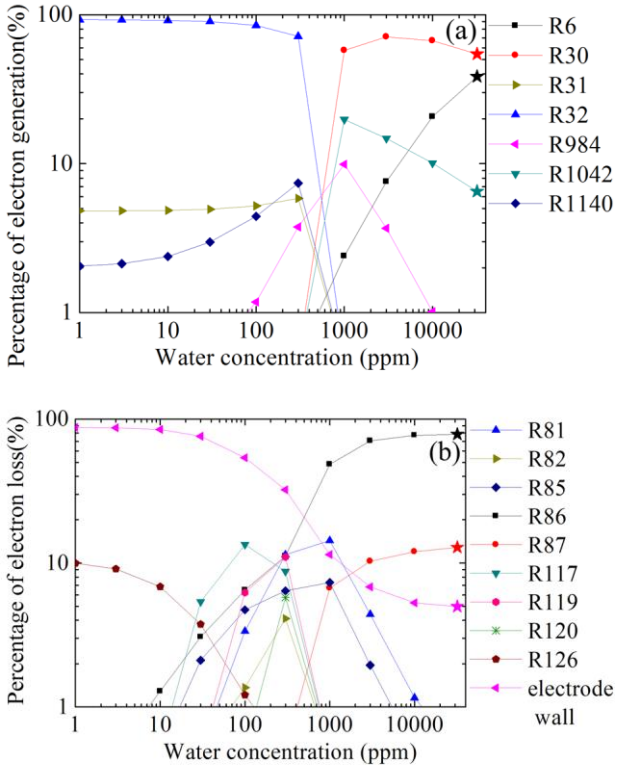

Figure 11. Main physicochemical pathways for (a) the production and (b) the loss of electrons as a function of the water content in the feed gas.

Atomic oxygen is an important reactive oxygen species produced in plasmas that is not easily obtained by other means. The main pathways for the generation and loss of ground state O are illustrated in Figure 12. Many reactions contribute to the generation and loss of O and most of them are driven by heavy particles instead that by electrons. At low water concentrations ($[H_2O]$<300 ppm) the main channel for the production of ground state O is collisional relaxation of $O(^1D)$ (R1056) followed by collisional dissociation of OH and O_2molecules by argon metastables (R1121,R1118 and R1125). The reactions are as follows:

$$Ar+O(^1D)\rightarrow O+Ar \quad (R1056)$$

$$Ar_2^*+OH\rightarrow H+O+2Ar \quad (R1121)$$

$$Ar_2^*+O_2\rightarrow 2O+2Ar \quad (R1118)$$

$$Ar(^4S)+O_2\rightarrow 2O+Ar \quad (R1125)$$

This is different from CAPs operated in other gas mixtures (e.g. $He+O_2$, $He+H_2O$) in which ground state atomic oxygen is mainly produced by electron impact dissociation of O_2[35,57]. In $Ar+H_2O$ CAPs the concentration of $O(^1D)$ is relatively large and the amount of O_2 present in the plasma is small and therefore the electron impact dissociation is not an important pathway for the production of atomic O. As the water content in the feed gas increases, more $O_2$is produced in the discharge (see Figure 8) and electron impact dissociation becomes increasingly important. However, the net production of O at high water concentration is dominated by heavy particle collisions (R1196 and 1169):

$$2OH\rightarrow H_2O+O \quad (R1196)$$

$$H+HO_2\rightarrow H_2O+O \quad (R1169)$$

Regarding the loss of ground state O (Figure 12(b)), the dominant pathways at low water concentrations ($[H_2O]$<300 ppm) are wall losses (electrode and radial losses) and electron-impact excitation (R38):

$$e+O\rightarrow O(^1D)+e \quad (R38)$$

However, at high water concentrations these pathways are not important because the density of ground state O decreases(Figure 8) and the increasing abundance of OH and HO_2quench O:

$$O+OH\rightarrow H+O_2 \quad (R1184)$$

$$O+HO_2\rightarrow OH+O_2 \quad (R1185)$$

Interestingly, OH and HO_2 also play an important role for the production of ground state O, indicating that the reactive species O, OH and HO_2 have a strong circular relation. This circular relation has also been found in $He+H_2O$ CAPs[57].

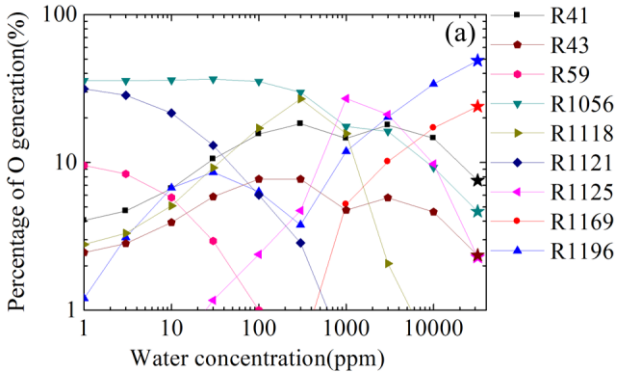

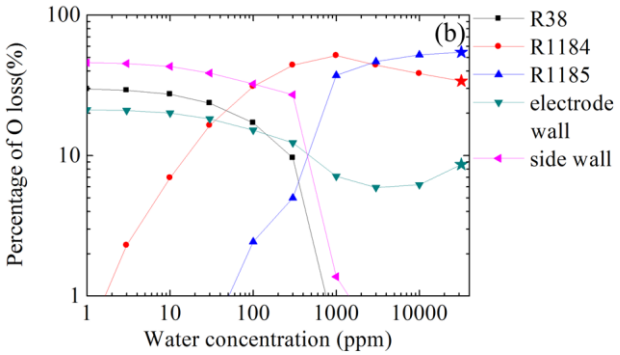

Figure 12. Main physicochemical pathways for (a) the production and (b) the loss of ground state O as a function of the water content in the feed gas.

Similarly to the production and loss of electrons and ground state O, the chemical pathways for the production and loss of OH have two distinct regimes (Figure 13). At low water concentrations ([H_2O]≤300 ppm), OH is mainly produced as a result of collisional dissociation of $H_2O$by argon dimer metastables (R1119). Other significant reactions in this regime include collisional dissociation of H_2O_2 by argon dimer metastable (R1120), charge transfer reaction (R848) and electron-impact dissociation (R70):

$$Ar_2^* + H_2O \rightarrow 2Ar + H + OH \quad (R1119)$$
$$Ar_2^* + H_2O_2 \rightarrow 2OH + 2Ar \quad (R1120)$$
$$Ar_2^+ + H_2O \rightarrow ArH^+ + OH + Ar \quad (R848)$$
$$e + H_2O_2 \rightarrow 2OH + e \quad (R70)$$

At higher water concentrations ([H_2O]>300 ppm), the density of argon dimers and dimer ions decrease rapidly (see Figures 4 and 7) and collisional dissociation of H_2O by atomic argon metastable (R1127), reaction between H and HO_2 (R1173) and collisional relaxation of OH(A) (R1108) become the dominant processes for OH production. Interestingly, electron impact dissociation of water molecules(R63), a key process in He+H_2O CAPs[15] and a process often believed to dominate the OH production[18], makes relatively small contribution (<10%) in Ar+H_2O CAPs:

$$H + HO_2 \rightarrow 2OH \quad (R1173)$$
$$Ar(^4S) + H_2O \rightarrow Ar + OH + H \quad (R1127)$$
$$Ar_2^* + H_2O \rightarrow 2Ar + H + OH \quad (R1119)$$
$$OH(A) + H_2O \rightarrow OH + H_2O \quad (R1108)$$
$$e + H_2O \rightarrow H + OH + e \quad (R63)$$

Regarding the loss of OH (Figure 13(b)), the dominant pathway at very low water concentrations is the loss through the walls (electrodes and radial loss). For water concentrations above 30 ppm, however, the concentration of water fragments in the plasma increases and volume reactions become increasingly important. The three-body reaction 2OH+Ar→H_2O_2+Ar (R1227) is the main OH loss pathway for water concentrations above 30 ppm. Reactions with other water fragments (R1155, R1184, R1197 and R1198) contribute significantly to the total loss of OH, particularly at high water concentrations:

$$2OH + Ar \rightarrow H_2O_2 + Ar \quad (R1227)$$
$$Ar + H + OH \rightarrow Ar + H_2O \quad (R1155)$$
$$O + OH \rightarrow H + O_2 \quad (R1184)$$
$$OH + HO_2 \rightarrow O_2 + H_2O \quad (R1197)$$
$$OH + H_2O_2 \rightarrow H_2O + HO_2 \quad (R1198)$$

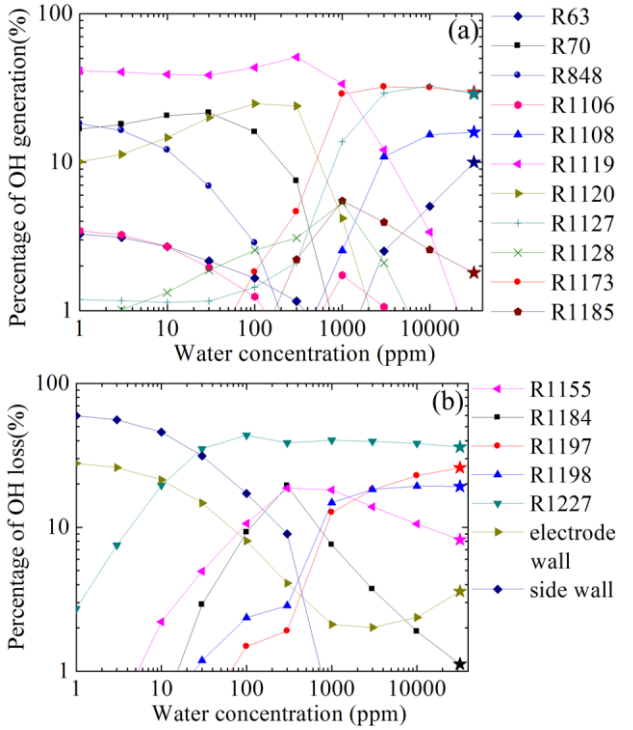

Figure 13.Main physicochemical pathways for (a) the production and (b) the loss of ground state OH as a function of the water content in the feed gas.

In Ref. [18] four chemical pathways were proposed as potential OH(A) production mechanisms in Ar+H_2O CAPs: electron excitation of OH, dissociative excitation of H_2O with argon metastables, dissociative electron excitation of H_2O and dissociative recombination of hydrated cations. According to our simulation results (Figure 14(a)), electron excitation of OH (R58: e+OH→OH(A)+e) is the dominant chemical process at low water concentrations ([H_2O]<300 ppm), whereas dissociative excitation of H_2O by argon metastables (R1159: Ar(^{4}S)+H_2O→Ar+H+OH(A)) is the dominant process at higher water concentrations. The other proposed chemical pathways are found to contribute less than 10% to the overall production of OH(A). Dissociative electron excitation of H_2O molecules (R67) is not very significant because at low water concentrations ([H_2O]<300 ppm) the concentration of OH is comparable to that of H_2O (Figure 8) and the energy required to excite OH to OH(A) is lower than the energy required to dissociate H_2O. At higher water concentrations the plasma becomes electronegative and the electron density is more than one order of magnitude smaller than the concentration of Ar(^{4}S) (see Figure 6 and 7) and the rate coefficient of R1159 is more than one order of magnitude larger than that of the

dissociative electron excitation of H_2O (R67).

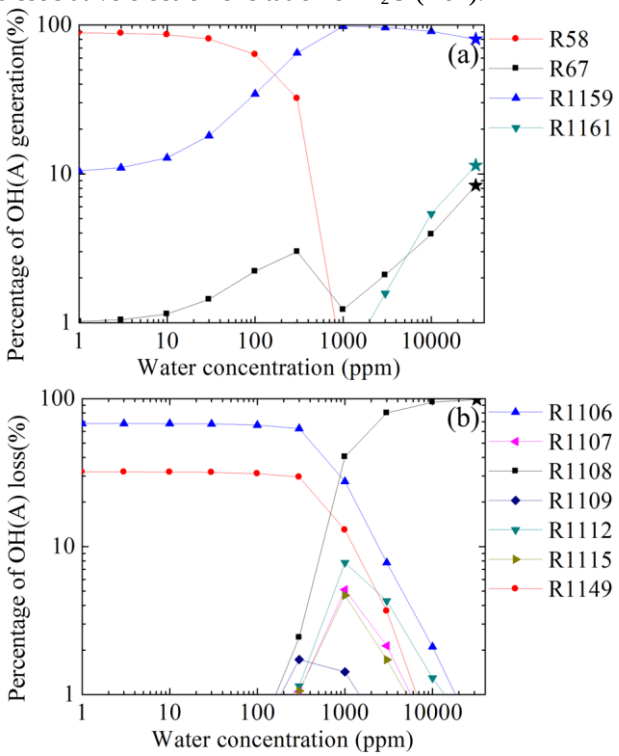

Figure 14. Main physicochemical pathways for (a) the production and (b) the loss of ground state OH(A) as a function of the water content in the feed gas.

Although the dissociative recombination of hydrated cations is not considered in the model due to the lack of data in the literature, we believe that this OH(A) production pathway[18] is likely to make only a very small contribution. Such reaction for all hydrated cations can be written as follows:

$$e + H^+(H_2O)_n \rightarrow OH(A) + 2H^+(n\text{-}1)H_2O$$

Taking $[H_2O]$=1000 ppm as an example, the electron density is ~3.9×10^{15} m^{-3}, and the total density of hydrated cations is ~3.1×10^{16} m^{-3}. Therefore the product of the densities is on the order of ~10^{32} m^{-6}. For this mechanism to be comparable to the OH(A) production via R58 and R1159 (~2.5×10^{23} $m^{-3}s^{-1}$), the reaction rate coefficient of the dissociative recombination above would need to be larger than 2.5×10^{-9} $m^{-3}s^{-1}$. Typically, however, electron-ion recombination rate coefficients are on the order of 10^{-13} $m^{-3}s^{-1}$,[108] i.e. four orders of magnitude lower than the one required for recombination of hydrated ions to make a significant contribution to the production of OH(A).

Regarding the loss of OH(A) (Figure 14(b)), the dominant reactions at low water concentration ($[H_2O]\leq300$ ppm) are the collisional relaxation (R1106) and radiative decay (R1149):

$$Ar+OH(A)\rightarrow Ar+OH \quad (R1106)$$
$$OH(A)\rightarrow OH+h\nu \quad (R1149)$$

At higher water concentration($[H_2O]>300$ ppm) collisional relaxation by water molecules (R1108) becomes the dominant loss process, while collisional relaxation by Ar, H_2,$O_2$and H_2O_2make relatively small contribution.:

$$OH(A)+H_2O\rightarrow H_2O+OH \quad (R1108)$$
$$Ar+OH(A)\rightarrow Ar+OH \quad (R1106)$$
$$OH(A)\rightarrow OH+h\nu \quad (R1149)$$
$$H_2+OH(A)\rightarrow H+H_2O \quad (R1112)$$
$$O_2+OH(A)\rightarrow O_2+OH \quad (R1107)$$
$$OH(A)+H_2O_2\rightarrow H_2O+HO_2 \quad (R1115)$$
$$H+OH(A)\rightarrow H_2+O \quad (R1109)$$

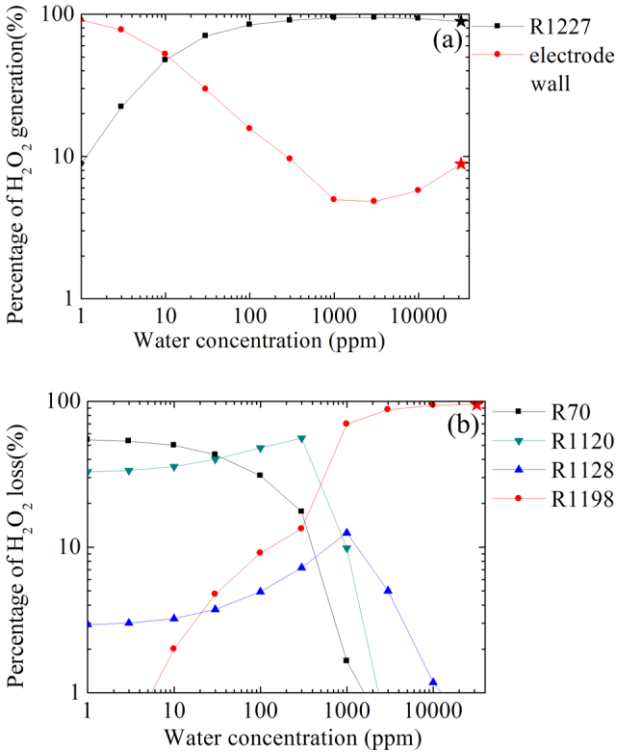

Figure 15. Main physicochemical pathways for (a) the production and (b) the loss of ground state H_2O_2 as a function of the water content in the feed gas.

As shown in Figure 15(a), the production of $H_2O_2$is dominated by the combination of two OH molecules in the volume reaction R1227 or on the electrode surfaces:

$$2OH+Ar\rightarrow H_2O_2+Ar \quad (R1227)$$

The main pathway for the loss of H_2O_2 are shown in Figure 15(b). At low water concentrations ($[H_2O]\leq300$ ppm) the dominant pathways are electron-impact dissociation (R70) and dissociation by collisions with argon dimer (R1120) and atomic argon metastables (R128).

$$e+H_2O_2\rightarrow 2OH+e \quad (R70)$$
$$Ar_2^*+H_2O_2\rightarrow 2OH+2Ar \quad (R1120)$$
$$Ar(^4S)+H_2O_2\rightarrow Ar+2OH \quad (R1128)$$
$$OH+H_2O_2\rightarrow H_2O+HO_2 \quad (R1198)$$

As the water concentration increases above 300 ppm, dissociation by collisions with OH molecules (R1198) become the dominant processes.

4. Concluding remarks

This paper reports on key species and chemical pathways in Ar+H_2O cold atmospheric-pressure plasmas. A global model incorporating 57 species and 1228 chemical reactions was used in the study and water vapor concentrations ranging from 1 ppm to saturation (32000 ppm) were considered. Although operation with water concentrations above ~6000 ppm results in unstable plasmas, it is recognized that in many applications plasmas are sustained in environments with a large humidity gradient and that near liquids and humid substrates the water content in the gas approaches saturation levels.

In contrast to He+H_2O plasmas[22,57,54], an abrupt transition in the properties of Ar+H_2O plasmas is found when the water concentration in the feed gas increases from 100 to 1000 ppm. At low water concentration ([H_2O]<300 ppm) most power is delivered to the electrons and the plasma is electropositive. Most water molecules in the plasma are dissociated in this regime. At higher water concentrations the plasma becomes electronegative and most power delivered to the plasma is coupled to ions. In this regime the plasma is less effective in generating reactive species and heavier hydrated ions become increasingly abundant.

The abrupt transition in species densities and chemical pathways observed when the water concentration increases from 100 to 1000 ppm is linked to the rapid change in the electron energy distribution function and thereby the electron-neutral excitation and ionization reaction rates. For example, the rate coefficient of the electron-impact ionization of argon atoms increases by more than 12 orders of magnitude.

This abrupt transition is not found in He+H_2O CAPs because when He is used as a carrier gas Penning processes dominate ionization processes. In Ar+H_2O CAPs, however, Penning processes are not possible because argon metastables (Ar(^{4}S): ~11.55 eV; Ar_2^*: ~10.8 eV) do not have enough energy to ionize other molecules (H_2O: ~12.62 eV). Instead, argon metastables contribute to dissociation of water molecules and play a fundamental role in step ionization processes.

Ar+H_2O CAPs are a good source of reactive oxygen species and in this paper key chemical process leading to the production and loss of O, OH, OH(A) and H_2O_2 have been discussed in detail, providing new insights and identifying differences with respect to better known He+H_2O CAPs. For example, OH production by electron impact dissociation of water molecules, a reaction dominating the production of OH in He+H_2O plasmas, is found to make negligible contribution to the production of OH in Ar+H_2O plasmas.

Acknowledgement

The authors would like to thank Dr. Ke Ding (Donghua University, P. R. China) for fruitful discussions related to this work. This work was supported by the National Science Foundation of China (Grant No. 51307134 and 51561065), the State Key Laboratory of Electrical Insulation and Power Equipment (No. EIPE14123), and the Fundamental Research Funds for the Central Universities.

Appendix

Number	Reaction	Rate coefficient[a,b]	Ref
Momentum transfer			
1	$e + Ar \rightarrow Ar + e$	$f(T_e)$	58
2	$e + H_2O \rightarrow e + H_2O$	$f(T_e)$	59
3	$e + H_2 \rightarrow H_2 + e$	$f(T_e)$	60
4	$e + O_2 \rightarrow O_2 + e$	$f(T_e)$	61
5	$e + OH \rightarrow OH + e$	$f(T_e)$	62c
Electron-impact Ionization			
6	$e + H_2O \rightarrow H_2O^+ + 2e$	$f(T_e)$	59
7	$e + H_2O \rightarrow OH^+ + H + 2e$	$f(T_e)$	59
8	$e + H_2O \rightarrow O^+ + H_2 + 2e$	$f(T_e)$	59
9	$e + H_2O \rightarrow H^+ + OH + 2e$	$f(T_e)$	59
10	$e + H_2O \rightarrow {H_2}^+ + O + 2e$	$f(T_e)$	59
11	$e + H \rightarrow H^+ + 2e$	$f(T_e)$	63
12	$e + H^- \rightarrow H + 2e$	$f(T_e)$	63
13	$e + H_2 \rightarrow {H_2}^+ + 2e$	$f(T_e)$	63
14	$e + H_2 \rightarrow H^+ + H + 2e$	$f(T_e)$	63
15	$e + O \rightarrow O^+ + 2e$	$f(T_e)$	72
16	$e + O\left({}^1D\right) \rightarrow O^+ + 2e$	$f(T_e)$	d
17	$e + O\left({}^1S\right) \rightarrow O^+ + 2e$	$f(T_e)$	d
18	$e + O^- \rightarrow O + 2e$	$1.95\times10^{-12} T_e^{\,0.5} \exp(-3.4/T_e)$	64
19	$e + O_2 \rightarrow {O_2}^+ + 2e$	$f(T_e)$	73
20	$e + O_2 \rightarrow O^+ + O + 2e$	$f(T_e)$	73
21	$e + O_2(a) \rightarrow {O_2}^+ + 2e$	$f(T_e)$	d
22	$e + O_2(a) \rightarrow O^+ + O + 2e$	$f(T_e)$	d
23	$e + O_2(b) \rightarrow {O_2}^+ + 2e$	$f(T_e)$	d
24	$e + O_2(b) \rightarrow O + O^+ + 2e$	$f(T_e)$	d
25	$e + OH \rightarrow OH^+ + 2e$	$f(T_e)$	62
26	$e + OH(A) \rightarrow OH^+ + 2e$	$3\times10^{-11} T_e^{\,2.61} \exp(-10.6/T_e)$	65
27	$e + OH^- \rightarrow OH + 2e$	$9.67\times10^{-6} T_e^{\,-1.89} \exp(-12.1/T_e)$	65
28	$e + H_2O_2 \rightarrow OH^+ + OH + 2e$	2.2×10^{-11}	66
29	$e + O_3 \rightarrow {O_2}^+ + O + 2e$	$f(T_e)$	67

30	$e + Ar \rightarrow Ar^{+} + 2e$	$f(T_e)$	68
31	$e + Ar\left(^4S\right) \rightarrow Ar^{+} + 2e$	$f(T_e)$	69
32	$e + Ar_2^{*} \rightarrow Ar_2^{+} + 2e$	$f(T_e)$	70
33	$e + Ar\left(^4P\right) \rightarrow Ar^{+} + 2e$	$f(T_e)$	69
Electron Impact Excitation & Dissociation & De-excitation			
34	$e + H_2 \rightarrow 2H + e$	$f(T_e)$	63
35	$e + H_2^{+} \rightarrow e + H^{+} + H$	$1.888\times10^{-7} T_e^{-0.13} \exp(-2.3/T_e)$	71
36	$e + H_3^{+} \rightarrow e + H^{+} + 2H$	$1.75\times10^{-8} T_e^{0.95} \exp(-10.5/T_e)$	63
37	$e + O \rightarrow O\left(^1S\right) + e$	$f(T_e)$	72
38	$e + O \rightarrow O\left(^1D\right) + e$	$f(T_e)$	72
39	$e + O_2 \rightarrow O_2(b) + e$	$f(T_e)$	61
40	$e + O_2 \rightarrow O_2(a) + e$	$f(T_e)$	61
41	$e + O_2 \rightarrow O\left(^1D\right) + O + e$	$f(T_e)$	73
42	$e + O_2 \rightarrow O\left(^1S\right) + O + e$	$f(T_e)$	74
43	$e + O_2 \rightarrow 2O + e$	$f(T_e)$	75
44	$e + O_2 \rightarrow O_2(v=1) + e$	$f(T_e)$	76
45	$e + O_2 \rightarrow O_2(v=2) + e$	$f(T_e)$	76
46	$e + O_2 \rightarrow O_2(v=3) + e$	$f(T_e)$	76
47	$e + O_2 \rightarrow O_2(v=4) + e$	$f(T_e)$	76
48	$e + O_3 \rightarrow O^{+} + O + O^{-} + e$	$f(T_e)$	67
49	$e + O_2(a) \rightarrow O_2(b) + e$	$f(T_e)$	77
50	$e + O_2(a) \rightarrow 2O + e$	$f(T_e)$	d
51	$e + O_2(a) \rightarrow O_2 + e$	$5.6\times10^{-9} \exp(-2.2/T_e)$	78
52	$e + O_2(a) \rightarrow O\left(^1D\right) + O + e$	$f(T_e)$	75
53	$e + O_2(a) \rightarrow O\left(^1S\right) + O + e$	$f(T_e)$	d
54	$e + O_2(b) \rightarrow O_2 + e$	$9.72\times10^{-10} \exp(-0.591/T_e)$	79
55	$e + O_2(b) \rightarrow 2O + e$	$f(T_e)$	d
56	$e + O_2(b) \rightarrow O\left(^1D\right) + O + e$	$f(T_e)$	d
57	$e + O_2(b) \rightarrow O\left(^1S\right) + O + e$	$f(T_e)$	d
58	$e + OH \rightarrow OH(A) + e$	$f(T_e)$	62k
59	$e + OH \rightarrow O + H + e$	$f(T_e)$	62k
60	$e + OH(A) \rightarrow O + H + e$	$1.5\times10^{-7} T_e^{-0.75} \exp(-3.9/T_e)$	65
61	$e + H_2O \rightarrow e + H_2O(v=100+001)$	$f(T_e)$	59

62	$e + H_2O \rightarrow e + H_2O(v = 010)$	$f(T_e)$	59
63	$e + H_2O \rightarrow H + OH + e$	$f(T_e)$	59
64	$e + H_2O \rightarrow H_2 + O + e$	$f(T_e)$	80
65	$e + H_2O \rightarrow O(^1D) + H_2 + e$	$f(T_e)$	80
66	$e + H_2O \rightarrow O(^1S) + H_2 + e$	$f(T_e)$	59
67	$e + H_2O \rightarrow OH(A) + H + e$	$f(T_e)$	59
68	$e + HO_2 \rightarrow O + OH + e$	1.67×10^{-9}	81
69	$e + HO_2 \rightarrow H + O_2 + e$	3.1×10^{-9}	81
70	$e + H_2O_2 \rightarrow 2OH + e$	2.36×10^{-9}	81
71	$e + H_2O_2 \rightarrow H + HO_2 + e$	3.1×10^{-11}	66
72	$e + O_3 \rightarrow O + O_2 + e$	$f(T_e)$	82
73	$e + Ar \rightarrow Ar(^4S) + e$	$f(T_e)$	83
74	$e + Ar \rightarrow Ar(^4P) + e$	$f(T_e)$	83
75	$e + Ar(^4S) \rightarrow Ar + e$	2×10^{-7}	84
76	$e + Ar(^4P) \rightarrow Ar + e$	$3.9\times10^{-10}T_e^{0.71}$	85
77	$e + Ar_2^* \rightarrow e + Ar + Ar(^4S)$	$1\times10^{-8}\exp(-1/T_e)$	86
Electron Impact Attachment & Dissociative Attachment			
78	$e + H \rightarrow H^-$	$3.46\times10^{-16}T_e^{0.5}$	87
79	$e + H_2 \rightarrow H + H^-$	$f(T_e)$	88
80	$e + O \rightarrow O^-$	$f(T_e)$	89
81	$e + O_2 \rightarrow O + O^-$	$f(T_e)$	74
82	$e + O_2(a) \rightarrow O + O^-$	$f(T_e)$	90
83	$e + OH \rightarrow OH^-$	1×10^{-15}	91
84	$e + H_2O_2 \rightarrow H_2O + O^-$	$f(T_e)$	92
85	$e + H_2O_2 \rightarrow OH + OH^-$	$f(T_e)$	92
86	$e + H_2O \rightarrow H^- + OH$	$f(T_e)$	59
87	$e + H_2O \rightarrow O^- + H_2$	$f(T_e)$	59
88	$e + H_2O \rightarrow OH^- + H$	$f(T_e)$	59
89	$e + O_3 \rightarrow O + O_2^-$	$f(T_e)$	74
90	$e + O_3 \rightarrow O^- + O_2$	$f(T_e)$	74
91	$e + 2O_2 \rightarrow O_2^- + O_2$	$2.26\times10^{-30}(T_g/300)^{-0.5}$	79
92	$e + O_2 + H_2O \rightarrow O_2^- + H_2O$	1.4×10^{-29}	93
93	$e + O_2 + Ar \rightarrow O_2^- + Ar$	1×10^{-31}	ab
94	$e + O_3 + M \rightarrow O_3^- + M$	1×10^{-31}	93

95	$e + O + O_2 \rightarrow O^- + O_2$	1×10^{-31}	93
96	$e + O + H_2O \rightarrow O^- + H_2O$	1.4×10^{-29}	r
97	$e + O + Ar \rightarrow O^- + Ar$	1×10^{-31}	s
98	$e + OH + Ar \rightarrow OH^- + Ar$	3×10^{-31}	ab
Dissociative recombination			
99	$e + H^+ \rightarrow H$	$2.62\times10^{-13}T_e^{-0.5}$	94
100	$2e + H_2^+ \rightarrow H_2 + e$	$7.18\times10^{-27}T_e^{-4.5}$	108
101	$e + H_2^+ \rightarrow H^+ + H^-$	$2.17\times10^{-10}T_e^{-0.2}\exp(-0.2/T_e)$	71
102	$e + H_3^+ \rightarrow 3H$	$4.15\times10^{-8}T_e^{-0.4}$	63
103	$e + O^+ \rightarrow O\left(^1D\right)$	$5.3\times10^{-13}T_e^{-0.5}$	64
104	$e + O_2^+ \rightarrow 2O$	$1.2\times10^{-8}T_e^{-0.7}$	64
105	$e + O_2^+ \rightarrow O + O\left(^1D\right)$	$8.88\times10^{-9}T_e^{-0.7}$	64
106	$e + O_2^+ \rightarrow 2O\left(^1D\right)$	$6.87\times10^{-9}T_e^{-0.7}$	93
107	$e + O_4^+ \rightarrow 2O_2$	$2.25\times10^{-7}T_e^{-0.5}$	108
108	$e + O_6^+ \rightarrow 3O_2$	$2.25\times10^{-7}T_e^{-0.5}$	108e
109	$e + OH^+ \rightarrow H + O$	$6\times10^{-9}T_e^{-0.5}$	87
110	$e + H_2O^+ \rightarrow H + OH$	$5.1\times10^{-8}T_e^{-0.5}$	95
111	$e + H_2O^+ \rightarrow H_2 + O$	$1.86\times10^{-8}T_e^{-0.5}$	95
112	$e + H_2O^+ \rightarrow 2H + O$	$2.32\times10^{-8}T_e^{-0.5}$	95
113	$e + H_3O^+ \rightarrow H_2O + H$	$5.63\times10^{-8}T_e^{-0.5}$	87
114	$e + H_3O^+ \rightarrow 2H + OH$	$1.05\times10^{-7}T_e^{-0.5}$	87
115	$e + H_2O_3^+ \rightarrow H_2O + O_2$	$7.22\times10^{-7}T_e^{-0.2}$	96
116	$e + H_4O_2^+ \rightarrow H_2O + OH + H$	$9.6\times10^{-7}T_e^{-0.2}$	96
117	$e + H_5O_2^+ \rightarrow 2H_2O + H$	$1.62\times10^{-6}T_e^{-0.15}$	96
118	$e + H_4O_4^+ \rightarrow 2H_2O + O_2$	$7.22\times10^{-7}T_e^{-0.2}$	121
119	$e + H_7O_3^+ \rightarrow H + 3H_2O$	$2.24\times10^{-6}T_e^{-0.08}$	97
120	$e + H_9O_4^+ \rightarrow H + 4H_2O$	3.6×10^{-6}	97
121	$e + H_{11}O_5^+ \rightarrow H + 5H_2O$	4×10^{-6}	98
122	$e + H_{13}O_6^+ \rightarrow H + 6H_2O$	4×10^{-6}	98
123	$e + H_{15}O_7^+ \rightarrow H + 7H_2O$	4×10^{-6}	98
124	$e + ArH^+ \rightarrow H + Ar$	1×10^{-7}	99
125	$e + Ar_2^+ \rightarrow Ar\left(^4S\right) + Ar$	$1\times10^{-8}T_e^{-0.6}(T_g/300)^{-0.6}$	100
126	$e + Ar_2^+ \rightarrow 2Ar$	$7.34\times10^{-8}T_e^{-0.67}(T_g/300)^{-0.58}$	101
127	$e + O^+ + M \rightarrow O + M$	$2.49\times10^{-29}T_e^{-1.5}$	108

128	$e + O_2^+ + M \rightarrow O_2 + M$	$2.49\times10^{-29} T_e^{-1.5}$	108
129	$e + O_4^+ + M \rightarrow 2O_2 + M$	$2.49\times10^{-29} T_e^{-1.5}$	108
130	$e + O_6^+ + M \rightarrow 3O_2 + M$	$2.49\times10^{-29} T_e^{-1.5}$	108
131	$e + H^+ + M \rightarrow H + M$	$2.49\times10^{-29} T_e^{-1.5}$	108
132	$e + H_2^+ + M \rightarrow H_2 + M$	$2.49\times10^{-29} T_e^{-1.5}$	108
133	$e + H_3^+ + M \rightarrow H_2 + H + M$	$2.49\times10^{-29} T_e^{-1.5}$	108
134	$e + OH^+ + M \rightarrow OH + M$	$2.49\times10^{-29} T_e^{-1.5}$	108
135	$e + HO_2^+ + M \rightarrow HO_2 + M$	$2.49\times10^{-29} T_e^{-1.5}$	108
136	$e + H_2O^+ + M \rightarrow H_2O + M$	$2.49\times10^{-29} T_e^{-1.5}$	108
137	$e + H_2O_2^+ + M \rightarrow H_2O + O + M$	$2.49\times10^{-29} T_e^{-1.5}$	108
138	$e + H_2O_3^+ + M \rightarrow H_2O + O_2 + M$	$2.49\times10^{-29} T_e^{-1.5}$	108
139	$e + H_4O_2^+ + M \rightarrow 2H_2O + M$	$2.49\times10^{-29} T_e^{-1.5}$	108
140	$e + H_4O_4^+ + M \rightarrow 2H_2O + O_2 + M$	$2.49\times10^{-29} T_e^{-1.5}$	108
141	$e + H_3O^+ + M \rightarrow H_2O + H + M$	$2.49\times10^{-29} T_e^{-1.5}$	108
142	$e + H_5O_2^+ + M \rightarrow 2H_2O + H + M$	$2.49\times10^{-29} T_e^{-1.5}$	108
143	$e + H_7O_3^+ + M \rightarrow 3H_2O + H + M$	$2.49\times10^{-29} T_e^{-1.5}$	108
144	$e + H_9O_4^+ + M \rightarrow 4H_2O + H + M$	$2.49\times10^{-29} T_e^{-1.5}$	108
145	$e + H_{11}O_5^+ + M \rightarrow 5H_2O + H + M$	$2.49\times10^{-29} T_e^{-1.5}$	108
146	$e + H_{13}O_6^+ + M \rightarrow 6H_2O + H + M$	$2.49\times10^{-29} T_e^{-1.5}$	108
147	$e + H_{15}O_7^+ + M \rightarrow 7H_2O + H + M$	$2.49\times10^{-29} T_e^{-1.5}$	108
148	$e + Ar^+ + M \rightarrow Ar + M$	$2.49\times10^{-29} T_e^{-1.5}$	81
149	$e + Ar_2^+ + M \rightarrow Ar\left({}^4S\right) + Ar + M$	$2.49\times10^{-29} T_e^{-1.5}$	102
150	$e + ArH^+ + M \rightarrow Ar + H + M$	$2.49\times10^{-29} T_e^{-1.5}$	81
151	$2e + Ar^+ \rightarrow Ar\left({}^4S\right) + e$	$7.18\times10^{-27} T_e^{-4.5}$	103
152	$2e + Ar^+ \rightarrow Ar + e$	7×10^{-27}	101
153	$2e + H^+ \rightarrow H + e$	$8.8\times10^{-27} T_e^{-4.5}$	104
154	$2e + O^+ \rightarrow O + e$	$5.12\times10^{-27} T_e^{-4.5}$	64
155	$2e + O_2^+ \rightarrow O_2 + e$	$7.18\times10^{-27} T_e^{-4.5}$	108
156	$2e + O_4^+ \rightarrow 2O_2 + e$	$7.18\times10^{-27} T_e^{-4.5}$	108
157	$2e + O_6^+ \rightarrow 3O_2 + e$	$7.18\times10^{-27} T_e^{-4.5}$	108e
158	$2e + H_5O_2^+ \rightarrow 2H_2O + H + e$	$5\times10^{-27} T_e^{-4.5}$	96
159	$2e + H_4O_2^+ \rightarrow H_2O + OH + H + e$	$5\times10^{-27} T_e^{-4.5}$	96
160	$2e + H_2O_3^+ \rightarrow H_2O + O_2 + e$	$5\times10^{-27} T_e^{-4.5}$	96
161	$2e + H_4O_4^+ \rightarrow 2H_2O + O_2 + e$	$5\times10^{-27} T_e^{-4.5}$	121

162	$2e + H_7O_3^+ \rightarrow 3H_2O + H + e$	$5\times10^{-27} T_e^{-4.5}$	i
163	$2e + H_9O_4^+ \rightarrow 4H_2O + H + e$	$5\times10^{-27} T_e^{-4.5}$	i
164	$2e + H_{11}O_5^+ \rightarrow 5H_2O + H + e$	$5\times10^{-27} T_e^{-4.5}$	i
Ion-ion recombination (Two-body reactions)			
165	$Ar^+ + O^- \rightarrow O + Ar$	2.7×10^{-7}	105
166	$Ar^+ + O_2^- \rightarrow O_2 + Ar$	$2\times10^{-7} (T_g / 300)^{-0.5}$	103
167	$Ar^+ + O_3^- \rightarrow O_3 + Ar$	$2\times10^{-7} (T_g / 300)^{-1}$	108
168	$ArH^+ + H^- \rightarrow H_2 + Ar$	1×10^{-7}	108
169	$ArH^+ + OH^- \rightarrow H_2O + Ar$	1×10^{-7}	108
170	$ArH^+ + O^- \rightarrow OH + Ar$	1×10^{-7}	108
171	$ArH^+ + O_2^- \rightarrow HO_2 + Ar$	1×10^{-7}	108
172	$Ar_2^+ + H^- \rightarrow H + 2Ar$	1×10^{-7}	108
173	$Ar_2^+ + O^- \rightarrow O + 2Ar$	1×10^{-7}	108
174	$Ar_2^+ + OH^- \rightarrow OH + 2Ar$	1×10^{-7}	108
175	$Ar_2^+ + O_2^- \rightarrow O_2 + 2Ar$	1×10^{-7}	108
176	$Ar_2^+ + O_3^- \rightarrow O_3 + 2Ar$	1×10^{-7}	108
177	$H^- + H_2^+ \rightarrow H + H_2$	$2\times10^{-7} (T_g / 300)^{-0.5}$	106
178	$H^- + H_3^+ \rightarrow 2H_2$	$2\times10^{-7} (T_g / 300)^{-0.5}$	107
179	$H^- + O^+ \rightarrow H + O$	$2.3\times10^{-7} (T_g / 300)^{-0.5}$	87
180	$H^- + O_2^+ \rightarrow H + O_2$	$2\times10^{-7} (T_g / 300)^{-0.5}$	108
181	$H^- + OH^+ \rightarrow H_2O$	$2\times10^{-7} (T_g / 300)^{-0.5}$	108
182	$O^- + H^+ \rightarrow H + O$	$2\times10^{-7} (T_g / 300)^{-0.5}$	108
183	$O^- + H_2^+ \rightarrow H_2O$	$2\times10^{-7} (T_g / 300)^{-0.5}$	108
184	$O^- + O^+ \rightarrow 2O$	$2\times10^{-7} (T_g / 300)^{-0.5}$	64
185	$O^- + O^+ \rightarrow O + O\left(^1D\right)$	$4.9\times10^{-10} (T_g / 300)^{-0.5}$	78
186	$O^- + O_2^+ \rightarrow O_2 + O$	$2\times10^{-7} (T_g / 300)^{-0.5}$	93
187	$O^- + O_4^+ \rightarrow 2O_2 + O$	1×10^{-7}	108
188	$O^- + OH^+ \rightarrow HO_2$	$2\times10^{-7} (T_g / 300)^{-0.5}$	108
189	$O_2^- + H^+ \rightarrow HO_2$	$2\times10^{-7} (T_g / 300)^{-0.5}$	108
190	$O_2^- + H_2^+ \rightarrow H_2 + O_2$	$2\times10^{-7} (T_g / 300)^{-0.5}$	108
191	$O_2^- + O^+ \rightarrow O_2 + O$	$2.7\times10^{-7} (T_g / 300)^{-0.5}$	79
192	$O_2^- + O_2^+ \rightarrow 2O_2$	$2\times10^{-7} (T_g / 300)^{-0.5}$	79,93

193	$O_2^- + O_2^+ \rightarrow O_2 + 2O$	$1.01\times10^{-7}(T_g/300)^{-0.5}$	79
194	$O_2^- + O_4^+ \rightarrow 3O_2$	1×10^{-7}	108
195	$O_2^- + OH^+ \rightarrow OH + O_2$	$2\times10^{-7}(T_g/300)^{-0.5}$	108
196	$O_3^- + O^+ \rightarrow O_3 + O$	$2.7\times10^{-7}(T_g/300)^{-0.5}$	64
197	$O_3^- + O_2^+ \rightarrow O_3 + 2O$	1×10^{-7}	64
198	$O_3^- + O_2^+ \rightarrow O_3 + O_2$	$2\times10^{-7}(T_g/300)^{-0.5}$	108
199	$O_3^- + O_4^+ \rightarrow 3O_2 + O$	1×10^{-7}	108
200	$OH^- + H_2^+ \rightarrow H_2O + H$	1×10^{-7}	108
201	$OH^- + H_3^+ \rightarrow H_2O + H_2$	$2\times10^{-7}(T_g/300)^{-0.5}$	108
202	$OH^- + O^+ \rightarrow HO_2$	$2\times10^{-7}(T_g/300)^{-0.5}$	108
203	$OH^- + O_2^+ \rightarrow OH + O_2$	$2\times10^{-7}(T_g/300)^{-0.5}$	108
204	$OH^- + OH^+ \rightarrow 2OH$	$2\times10^{-7}(T_g/300)^{-0.5}$	108
205	$H_2O^+ + H^- \rightarrow 2H + OH$	$2\times10^{-7}(T_g/300)^{-0.5}$	108
206	$H_2O^+ + H^- \rightarrow H + H_2O$	$2\times10^{-7}(T_g/300)^{-0.5}$	108
207	$H_2O^+ + O^- \rightarrow O + H_2O$	$2\times10^{-7}(T_g/300)^{-0.5}$	108
208	$H_2O^+ + O^- \rightarrow O + H + OH$	1×10^{-7}	108
209	$H_2O^+ + O_2^- \rightarrow H_2O + O_2$	$2\times10^{-7}(T_g/300)^{-0.5}$	108
210	$H_2O^+ + O_2^- \rightarrow OH + H + O_2$	1×10^{-7}	108
211	$H_2O^+ + O_2^- \rightarrow H_2O + 2O$	1×10^{-7}	108
212	$H_2O^+ + O_2^- \rightarrow OH + H + 2O$	1×10^{-7}	108
213	$H_2O^+ + O_3^- \rightarrow O_3 + H_2O$	$2\times10^{-7}(T_g/300)^{-0.5}$	108
214	$H_2O^+ + O_3^- \rightarrow O + O_2 + H_2O$	1×10^{-7}	108
215	$H_2O^+ + O_3^- \rightarrow O_3 + H + OH$	1×10^{-7}	108
216	$H_2O^+ + O_3^- \rightarrow O + O_2 + H + OH$	1×10^{-7}	108
217	$H_2O^+ + OH^- \rightarrow H_2O + OH$	$2\times10^{-7}(T_g/300)^{-0.5}$	108
218	$H_2O^+ + OH^- \rightarrow H + O + H_2O$	1×10^{-7}	108
219	$H_2O^+ + OH^- \rightarrow 2OH + H$	1×10^{-7}	108
220	$H_2O^+ + OH^- \rightarrow 2H + O + OH$	1×10^{-7}	108
221	$H_3O^+ + H^- \rightarrow OH + H_2 + H$	$2.3\times10^{-7}(T_g/300)^{-0.5}$	87
222	$H_3O^+ + H^- \rightarrow H_2O + H_2$	$2.3\times10^{-7}(T_g/300)^{-0.5}$	87
223	$H_3O^+ + H^- \rightarrow H_2O + 2H$	1×10^{-7}	108
224	$H_3O^+ + O^- \rightarrow H_2O + OH$	$2\times10^{-7}(T_g/300)^{-0.5}$	108

225	$H_3O^+ + O^- \rightarrow H_2O + O + H$	1×10^{-7}	108
226	$H_3O^+ + O_2^- \rightarrow H_2O + O_2 + H$	1×10^{-7}	108
227	$H_3O^+ + O_3^- \rightarrow O_3 + H + H_2O$	1×10^{-7}	108
228	$H_3O^+ + O_3^- \rightarrow O + O_2 + H + H_2O$	1×10^{-7}	108
229	$H_3O^+ + OH^- \rightarrow 2H_2O$	$4\times10^{-7}(T_g/300)^{-0.5}$	109
230	$H_3O^+ + OH^- \rightarrow H_2O + H + OH$	1×10^{-7}	108
231	$H_3O^+ + OH^- \rightarrow H_2O + 2H + O$	1×10^{-7}	108
232	$HO_2^+ + H^- \rightarrow HO_2 + H$	$2\times10^{-7}(T_g/300)^{-0.5}$	108
233	$HO_2^+ + O^- \rightarrow HO_2 + O$	$2\times10^{-7}(T_g/300)^{-0.5}$	108
234	$HO_2^+ + O_2^- \rightarrow HO_2 + O_2$	$2\times10^{-7}(T_g/300)^{-0.5}$	108
235	$HO_2^+ + O_2^- \rightarrow HO_2 + 2O$	1×10^{-7}	108
236	$HO_2^+ + O_3^- \rightarrow HO_2 + O_3$	$2\times10^{-7}(T_g/300)^{-0.5}$	108
237	$HO_2^+ + O_3^- \rightarrow HO_2 + O + O_2$	1×10^{-7}	108
238	$HO_2^+ + OH^- \rightarrow HO_2 + OH$	$2\times10^{-7}(T_g/300)^{-0.5}$	108
239	$HO_2^+ + OH^- \rightarrow HO_2 + H + O$	1×10^{-7}	108
Ion-ion recombination (Two-body reactions)(most clusters)			
240-299	$A^+(H_2O)_n + B^- \rightarrow nH_2O + A + B$ $A^+(H_2O)_n \rightarrow H_5O_2^+, H_4O_2^+, H_2O_3^+, H_7O_3^+,$ $H_9O_4^+, H_{11}O_5^+, H_{13}O_6^+, H_{15}O_7^+, H_2O_2^+,$ $H_4O_4^+, O_4^+, O_6^+$ $B^- \rightarrow H^-, OH^-, O^-, O_2^-, O_3^-$	1×10^{-7}	108
300-389	$A^+ + B^-(H_2O)_n \rightarrow nH_2O + A + B$ $A^+ \rightarrow Ar^+, ArH^+, Ar_2^+, H^+, H_2^+, H_3^+, O^+, O_2^+$ $, OH^+, HO_2^+$ $B^-(H_2O)_n \rightarrow H_2O_2^-, H_2O_3^-, H_2O_4^-, H_3O_2^-,$ $H_5O_3^-, H_4O_4^-, H_6O_5^-, H_4O_5^-, O_4^-$	1×10^{-7}	108
390-501	$A^+(H_2O)_m + B^-(H_2O)_n \rightarrow (m+n)H_2O + A +$ $A^+(H_2O)_m \rightarrow H_5O_2^+, H_4O_2^+, H_2O_3^+, H_7O_3^+,$ $H_9O_4^+, H_{11}O_5^+, H_{13}O_6^+, H_{15}O_7^+, H_2O_2^+,$ $H_4O_4^+, H_2O_2^+, H_4O_4^+, O_4^+, O_6^+$ $B^-(H_2O)_n \rightarrow H_2O_2^-, H_2O_3^-, H_2O_4^-, H_3O_2^-, H$ $, H_4O_4^-, H_6O_5^-, H_4O_5^-, O_4^-$	1×10^{-7}	108

Ion-ion recombination (There-body reactions)			
502-556	$A^+ + B^- + M \rightarrow A + B + M$ $A^+ \rightarrow Ar^+, ArH^+, {Ar_2}^+, H^+, {H_2}^+, {H_3}^+, O^+, {O_2}^+$ $, OH^+, {HO_2}^+, {H_2O}^+$ $B^- \rightarrow H^-, O^-, OH^-, {O_2}^-, {O_3}^-$	$2\times10^{-25}(T_g/300)^{-2.5}$	108
557-621	$A^+(H_2O)_n + B^- + M \rightarrow nH_2O + A + B + M$ $A^+(H_2O)_n \rightarrow H_3O^+, {H_5O_2}^+, {H_4O_2}^+, {H_2O_3}^+,$ ${H_7O_3}^+, {H_9O_4}^+, {H_{11}O_5}^+, {H_{13}O_6}^+, {H_{15}O_7}^+, H_2O_2$ $, {H_4O_4}^+, {O_4}^+, {O_6}^+$ $B^- \rightarrow H^-, OH^-, O^-, {O_2}^-, {O_3}^-$	$2\times10^{-25}(T_g/300)^{-2.5}$	108
622-720	$A^+ + B^-(H_2O)_n + M \rightarrow nH_2O + A + B + M$ $A^+ \rightarrow Ar^+, ArH^+, {Ar_2}^+, H^+, {H_2}^+, {H_3}^+, O^+, {O_2}^+$ $, OH^+, {HO_2}^+, {H_2O}^+$ $B^-(H_2O)_n \rightarrow {H_2O_2}^-, {H_2O_3}^-, {H_2O_4}^-, {H_3O_2}^-,$ ${H_5O_3}^-, {H_4O_4}^-, {H_6O_5}^-, {H_4O_5}^-, {O_4}^-$	$2\times10^{-25}(T_g/300)^{-2.5}$	108
721-837	$A^+(H_2O)_m + B^-(H_2O)_n + M \rightarrow$ $(m+n)H_2O + A + B + M$ $A^+(H_2O)_m \rightarrow H_3O^+, {H_5O_2}^+, {H_4O_2}^+,$ ${H_2O_3}^+, {H_7O_3}^+, {H_9O_4}^+, {H_{11}O_5}^+, {H_{13}O_6}^+$ $, {H_{15}O_7}^+, {H_2O_2}^+, {H_4O_4}^+, {O_4}^+, {O_6}^+$ $B^-(H_2O)_n \rightarrow {H_2O_2}^-, {H_2O_3}^-, {H_2O_4}^-, {H_3O_2}^-,$ ${H_5O_3}^-, {H_4O_4}^-, {H_6O_5}^-, {H_4O_5}^-, {O_4}^-$	$2\times10^{-25}(T_g/300)^{-2.5}$	108
Charge transfer(Two-body reactions)			
840	$Ar^+ + H_2 \rightarrow ArH^+ + H$	8.8×10^{-10}	110
841	$Ar^+ + H_2 \rightarrow {H_2}^+ + Ar$	1.78×10^{-11}	119
842	$Ar^+ + O \rightarrow O^+ + Ar$	6.4×10^{-12}	111
843	$Ar^+ + O_2 \rightarrow {O_2}^+ + Ar$	$6.3\times10^{-11}(T_g/300)^{-0.78}$	112
844	$Ar^+ + H_2O \rightarrow ArH^+ + OH$	4.41×10^{-10}	113
845	$Ar^+ + H_2O \rightarrow {H_2O}^+ + Ar$	1.66×10^{-9}	119
846	${Ar_2}^+ + H_2 \rightarrow ArH^+ + H + Ar$	4.7×10^{-10}	110
847	${Ar_2}^+ + O_2 \rightarrow {O_2}^+ + 2Ar$	1.2×10^{-10}	116

848	$Ar_2^+ + H_2O \rightarrow ArH^+ + OH + Ar$	2.0×10^{-9}	114
849	$Ar_2^+ + H_2O \rightarrow H_2O^+ + 2Ar$	1.6×10^{-9}	115
850	$ArH^+ + H_2O \rightarrow H_3O^+ + Ar$	4.5×10^{-9}	116
851	$ArH^+ + H_2 \rightarrow H_3^+ + Ar$	3.5×10^{-10}	72
852	$ArH^+ + O_2 \rightarrow HO_2^+ + Ar$	6×10^{-10}	119
853	$H_2O^+ + O \rightarrow O_2^+ + H_2$	5.5×10^{-11}	138
854	$H_2O^+ + O_2 \rightarrow H_2O + O_2^+$	3.3×10^{-10}	93
855	$H_2O^+ + OH \rightarrow H_3O^+ + O$	6.9×10^{-10}	87
856	$H_2O^+ + H_2O \rightarrow H_3O^+ + OH$	1.85×10^{-9}	93
857	$H_2O^+ + H_2 \rightarrow H_3O^+ + H$	1.3×10^{-9}	117
858	$H^- + H_2O \rightarrow OH^- + H_2$	3.8×10^{-9}	87
859	$H^+ + O \rightarrow O^+ + H$	$7\times10^{-10}\exp(-232/T_e)$	87
860	$H^+ + O_2 \rightarrow O_2^+ + H$	2×10^{-9}	87
861	$H^+ + OH \rightarrow OH^+ + H$	2.1×10^{-9}	87
862	$H^+ + H_2O \rightarrow H_2O^+ + H$	6.9×10^{-9}	87
863	$H^+ + 2H_2 \rightarrow H_3^+ + H_2$	$3.1\times10^{-29}(T_g/300)^{-0.5}$	107
864	$H_2^+ + H \rightarrow H^+ + H_2$	6.39×10^{-10}	78
865	$H_2^+ + O \rightarrow OH^+ + H$	1.5×10^{-9}	87
866	$H_2^+ + O_2 \rightarrow O_2^+ + H_2$	8×10^{-10}	87
867	$H_2^+ + OH \rightarrow OH^+ + H_2$	7.6×10^{-10}	87
868	$H_2^+ + OH \rightarrow H_2O^+ + H$	7.6×10^{-10}	87
869	$H_2^+ + H_2O \rightarrow H_2O^+ + H_2$	3.9×10^{-9}	87
870	$H_2^+ + H_2O \rightarrow H_3O^+ + H$	3.4×10^{-9}	87
871	$H_2^+ + H_2 \rightarrow H_3^+ + H$	2.1×10^{-9}	107
872	$H_2^+ + Ar \rightarrow ArH^+ + H$	2.1×10^{-9}	118
873	$H_2^+ + O_2 \rightarrow HO_2^+ + H$	1.9×10^{-9}	119
874	$H_3^+ + O \rightarrow OH^+ + H_2$	8×10^{-10}	87
875	$H_3^+ + OH \rightarrow H_2O^+ + H_2$	1.3×10^{-9}	87
876	$H_3^+ + H_2O \rightarrow H_3O^+ + H_2$	5.9×10^{-9}	87
877	$H_3^+ + O_2 \rightarrow HO_2^+ + H_2$	6.7×10^{-10}	119
878	$O^+ + H \rightarrow H^+ + O$	6.8×10^{-10}	87
879	$O^+ + H_2 \rightarrow OH^+ + H$	1.62×10^{-9}	93
880	$O^+ + O_2 \rightarrow O_2^+ + O$	$2\times10^{-11}(T_g/300)^{-0.5}$	78
881	$O^+ + OH \rightarrow OH^+ + O$	3.3×10^{-10}	138

882	$O^+ + OH \rightarrow O_2^+ + H$	3.6×10^{-10}	138
883	$O^+ + H_2O \rightarrow H_2O^+ + O$	2.6×10^{-9}	93
884	$O_2^+ + O\left(^1D\right) \rightarrow O_2\left(a\right) + O^+$	$1\times10^{-12}(T_g/300)^{-0.5}$	78
885	$O_2^+ + H_2O_2 \rightarrow H_2O_2^+ + O_2$	1.5×10^{-9}	119
886	$OH^+ + H_2 \rightarrow H_2O^+ + H$	1.3×10^{-9}	138
887	$OH^+ + O \rightarrow H + O_2^+$	7.1×10^{-10}	87
888	$OH^+ + O_2 \rightarrow OH + O_2^+$	3.8×10^{-10}	93
889	$OH^+ + OH \rightarrow H_2O^+ + O$	7×10^{-10}	138
890	$OH^+ + H_2O \rightarrow H_2O^+ + OH$	1.5×10^{-9}	138
891	$OH^+ + H_2O \rightarrow H_3O^+ + O$	1.3×10^{-9}	119
892	$O_4^+ + Ar\left(^4S\right) \rightarrow O^+ + O + O_2 + Ar$	1×10^{-10}	ab
893	$O_4^+ + Ar_2^* \rightarrow O^+ + O + O_2 + 2Ar$	1×10^{-10}	ab
894	$O_4^+ + O \rightarrow O_2^+ + O_3$	3×10^{-10}	108
895	$O_4^+ + O\left(^1D\right) \rightarrow O_2^+ + O_2 + O$	3×10^{-10}	120
896	$O_4^+ + O\left(^1S\right) \rightarrow O_2^+ + O_2 + O$	3×10^{-10}	120
897	$O_4^+ + H_2O \rightarrow H_2O_3^+ + O_2$	1.7×10^{-9}	121
898	$O_4^+ + O_2 \rightarrow O_2^+ + 2O_2$	$3.3\times10^{-6}(T_g/300)^{-4}\exp(-5030/T_g)$	108
899	$O_4^+ + O_2\left(a\right) \rightarrow O_2^+ + 2O_2$	1×10^{-10}	108
900	$O_4^+ + O_2\left(b\right) \rightarrow O_2^+ + 2O_2$	1×10^{-10}	108
901	$O_4^+ + Ar \rightarrow O_2^+ + O_2 + Ar$	3×10^{-17}	ab
902	$HO_2^+ + H_2 \rightarrow H_3^+ + O_2$	3.3×10^{-10}	119
903	$H_2O_2^+ + H_2O \rightarrow H_3O^+ + HO_2$	1.7×10^{-9}	119
904	$H_2O_3^+ + H_2O \rightarrow H_4O_2^+ + O_2$	1×10^{-9}	96
905	$H_2O_3^+ + H_2O \rightarrow H_3O^+ + OH + O_2$	3×10^{-10}	122
906	$H_2O_3^+ + O_2\left(a\right) \rightarrow O_2^+ + O_2 + H_2O$	1×10^{-10}	96
907	$H_2O_3^+ + Ar \rightarrow O_2^+ + H_2O + Ar$	$1.24\times10^{-5}(T_g/300)^{-4}\exp(-7610/T_g)$	124
908	$H_4O_2^+ + H_2O \rightarrow H_5O_2^+ + OH$	1.4×10^{-9}	96
909	$H_4O_4^+ + Ar\left(^4S\right) \rightarrow 2H_2O + O + O^+ + Ar$	1×10^{-10}	ab
910	$H_4O_4^+ + Ar_2^* \rightarrow 2H_2O + O + O^+ + 2Ar$	1×10^{-10}	ab
911	$H_4O_4^+ + H_2O \rightarrow H_5O_2^+ + OH + O_2$	6.3×10^{-11}	123
912	$H_5O_2^+ + Ar \rightarrow H_3O^+ + H_2O + Ar$	6.3×10^{-15}	133
913	$H_7O_3^+ + Ar \rightarrow H_5O_2^+ + H_2O + Ar$	1.1×10^{-15}	133

914	$H_9O_4^+ + Ar \rightarrow H_7O_3^+ + H_2O + Ar$	1.8×10^{-16}	133
915	$H_{11}O_5^+ + Ar \rightarrow H_9O_4^+ + H_2O + Ar$	1.4×10^{-15}	133
916	$H_{11}O_5^+ + H_2O \rightarrow H_{13}O_6^+$	$7.28\times10^{-10}\times(2.54\times(T_g/300)^{-0.5}+0.62)$	124
917	$H_{13}O_6^+ \rightarrow H_{11}O_5^+ + H_2O$	$6.07\times10^{14}\times(2.54\times(T_g/300)^{-0.5}+0.62)\times\exp(-5000/T_g)$	124
918	$H_{13}O_6^+ + H_2O \rightarrow H_{15}O_7^+$	$7.18\times10^{-10}\times(2.54\times(T_g/300)^{-0.5}+0.62)$	124
919	$H_{15}O_7^+ \rightarrow H_{13}O_6^+ + H_2O$	$7.33\times10^{14}\times(2.54\times(T_g/300)^{-0.5}+0.62)\times\exp(-5000/T_g)$	124
920	$O^- + O_3 \rightarrow O_3^- + O$	$1.99\times10^{-10}(T_g/300)^{0.5}$	64
921	$O^- + H_2 \rightarrow OH^- + H$	3×10^{-11}	87
922	$O^- + O_2(a) \rightarrow O_2^- + O$	$1.1\times10^{-11}(T_g/300)^{-0.5}$	78
923	$O^- + H_2O \rightarrow OH^- + OH$	1.4×10^{-9}	125
924	$O_2^- + O_3 \rightarrow O_3^- + O_2$	$6\times10^{-10}(T_g/300)^{0.5}$	64
925	$O_2^- + OH \rightarrow OH^- + O_2$	1×10^{-10}	126
926	$O_2^- + O \rightarrow O^- + O_2$	$1.5\times10^{-10}(T_g/300)^{0.5}$	64
927	$O_3^- + Ar(^4S) \rightarrow O + O_2 + Ar + e$	3×10^{-10}	ab
928	$O_3^- + Ar_2^* \rightarrow O + O_2 + 2Ar + e$	3×10^{-10}	ab
929	$O_3^- + O \rightarrow 2O_2 + e$	1×10^{-11}	120
930	$O_3^- + O(^1D) \rightarrow O^- + O + O_2$	1×10^{-10}	120
931	$O_3^- + O(^1S) \rightarrow O + O_3 + e$	1×10^{-10}	120
932	$O_3^- + O(^1S) \rightarrow O^- + O + O_2$	1×10^{-10}	120
933	$O_3^- + O(^1S) \rightarrow O_2^- + 2O$	1×10^{-10}	120
934	$O_3^- + O_2(b) \rightarrow O^- + 2O_2$	1×10^{-10}	120
935	$O_3^- + O \rightarrow O_2^- + O_2$	$2.5\times10^{-10}(T_g/300)^{0.5}$	64
936	$O_3^- + H \rightarrow OH^- + O_2$	8.4×10^{-10}	127
937	$O_2^- + 2O_2 \rightarrow O_4^- + O_2$	$3.5\times10^{-31}(T_g/300)^{-1}$	120
938	$O_4^- + O_2(b) \rightarrow 3O_2 + e$	1×10^{-10}	120
939	$O_4^- + M \rightarrow O_2^- + O_2 + M$	$1\times10^{-10}\exp(-1044/T_g)$	108
940	$O_4^- + O \rightarrow O_3^- + O_2$	4×10^{-10}	108
941	$O_4^- + O \rightarrow O^- + 2O_2$	4×10^{-10}	108
942	$O_4^- + O(^1D) \rightarrow O_2^- + O_2 + O$	1×10^{-10}	120

943	$O_4^- + O(^1S) \rightarrow O^- + 2O_2$	1×10^{-10}	120
944	$O_4^- + O_2(a) \rightarrow O_2^- + 2O_2$	1×10^{-10}	108
945	$O_4^- + O_2(b) \rightarrow O_2^- + 2O_2$	1×10^{-10}	108
946	$O_4^- + O_3 \rightarrow O_3^- + 2O_2$	3×10^{-10}	120
947	$O_4^- + H_2O \rightarrow H_2O_3^- + O_2$	1.5×10^{-9}	128
948	$OH^- + O_3 \rightarrow OH + O_3^-$	$9\times10^{-10}(T_g/300)^{0.5}$	93
949	$H_2O_2^- + O_2 \rightarrow O_3^- + H_2O$	1×10^{-11}	129
950	$H_2O_2^- + H_2O \rightarrow H_3O_2^- + OH$	2×10^{-10}	128
951	$H_2O_3^- + O_3 \rightarrow O_3^- + O_2 + H_2O$	8×10^{-10}	129
952	$H_2O_3^- + O_2(a) \rightarrow O_2^- + O_2 + H_2O$	1×10^{-10}	120
953	$H_2O_3^- + O_2(b) \rightarrow O_2^- + O_2 + H_2O$	1×10^{-10}	120
954	$H_2O_3^- + O(^1D) \rightarrow O_2^- + O + H_2O$	1×10^{-10}	120
955	$H_2O_3^- + O(^1S) \rightarrow O_2^- + O + H_2O$	1×10^{-10}	120
956	$H_4O_4^- + M \rightarrow H_2O_3^- + H_2O + M$	1.1×10^{-14}	129
957	$H_4O_4^- + O_3 \rightarrow H_2O_4^- + H_2O + O_2$	7.8×10^{-10}	129
958	$H_6O_5^- + M \rightarrow H_4O_4^- + H_2O + M$	1.3×10^{-16}	128
959	$H_6O_5^- + O_3 \rightarrow H_4O_5^- + H_2O + O_2$	6.4×10^{-10}	128
Charge transfer(There-body reactions)			
960	$Ar^+ + 2Ar \rightarrow Ar_2^+ + Ar$	2.25×10^{-31}	130
961	$H^+ + H + M \rightarrow H_2^+ + M$	1×10^{-34}	131
962	$H^+ + H_2 + M \rightarrow H_3^+ + M$	1.5×10^{-29}	ab
963	$O^+ + O + M \rightarrow O_2^+ + M$	$1\times10^{-29}(T_g/300)^{0.5}$	64
964	$O_2^+ + H_2O + M \rightarrow H_2O_3^+ + M$	2×10^{-28}	132
965	$O_2^+ + 2O_2 \rightarrow O_4^+ + O_2$	$2.4\times10^{-30}(T_g/300)^{-3.2}$	108
966	$O_2^+ + O_2 + Ar \rightarrow O_4^+ + Ar$	$5.1\times10^{-31}(T_g/300)^{-3.1}$	ab
967	$O_4^+ + O_2 + M \rightarrow O_6^+ + M$	7×10^{-32}	123f
968	$H_2O_3^+ + H_2O + M \rightarrow H_4O_4^+ + M$	1.3×10^{-27}	121
969	$H_3O^+ + H_2O + M \rightarrow H_5O_2^+ + M$	1.9×10^{-28}	133
970	$H_5O_2^+ + H_2O + M \rightarrow H_7O_3^+ + M$	8.4×10^{-29}	133
971	$H_7O_3^+ + H_2O + M \rightarrow H_9O_4^+ + M$	3×10^{-29}	133
972	$O^- + O_2 + M \rightarrow O_3^- + M$	$1.1\times10^{-30}(T_g/300)^{-1}$	120
973	$O^- + H_2O + M \rightarrow H_2O_2^- + M$	1.3×10^{-28}	ab

974	$O_2^- + H_2O + M \rightarrow H_2O_3^- + M$	$3\times10^{-28}(T_g/300)^{-1}$	120
975	$O_2^- + O_2 + M \rightarrow O_4^- + M$	$3.5\times10^{-31}(T_g/300)^{-1}$	ab
976	$O_3^- + H_2O + M \rightarrow H_2O_4^- + M$	2.7×10^{-28}	129
977	$OH^- + H_2O + M \rightarrow H_3O_2^- + M$	2.5×10^{-28}	ab
978	$H_2O_4^- + H_2O + M \rightarrow H_4O_5^- + M$	1×10^{-28}	134
979	$H_3O_2^- + H_2O + M \rightarrow H_5O_3^- + M$	3.5×10^{-28}	ab
980	$H_4O_4^- + H_2O + M \rightarrow H_6O_5^- + M$	8.3×10^{-31}	123
981	$H_9O_4^+ + H_2O + M \rightarrow H_{11}O_5^+ + M$	7.4×10^{-30}	133
Collisional detachment			
982	$H^- + H \rightarrow H_2 + e$	1.3×10^{-9}	87
983	$H^- + O \rightarrow OH + e$	1×10^{-9}	87
984	$H^- + O_2 \rightarrow HO_2 + e$	1.2×10^{-9}	135
985	$H^- + OH \rightarrow H_2O + e$	1×10^{-10}	87
986	$H^- + Ar\left(^4S\right) \rightarrow Ar + H + e$	1×10^{-10}	z
987	$H^- + Ar\left(^4P\right) \rightarrow Ar + H + e$	1×10^{-10}	t
988	$H^- + Ar_2^* \rightarrow 2Ar + H + e$	1×10^{-10}	z
989	$O^- + H \rightarrow OH + e$	5×10^{-10}	87
990	$O^- + H_2 \rightarrow H_2O + e$	$6\times10^{-10}(T_g/300)^{-0.24}$	136
991	$O^- + O \rightarrow O_2 + e$	$2\times10^{-10}(T_g/300)^{0.5}$	64
992	$O^- + O_2(b) \rightarrow O_2 + O + e$	$6.9\times10^{-10}(T_g/300)^{0.5}$	64
993	$O^- + H_2O \rightarrow H_2O_2 + e$	5×10^{-13}	137
994	$O^- + O_2(a) \rightarrow O_3 + e$	$3\times10^{-10}(T_g/300)^{0.5}$	64
995	$O^- + O_2 \rightarrow O_3 + e$	$5\times10^{-15}(T_g/300)^{0.5}$	64
996	$O^- + O_3 \rightarrow 2O_2 + e$	$3.01\times10^{-10}(T_g/300)^{0.5}$	64
997	$O^- + O_3 \rightarrow O_2 + O_2^-$	$1.02\times10^{-11}(T_g/300)^{0.5}$	64
998	$O^- + Ar \rightarrow Ar + O + e$	$2.5\times10^{-18}(T_g/300)^{0.6}$	ab
999	$O^- + Ar\left(^4S\right) \rightarrow Ar + O + e$	3×10^{-10}	ab
1000	$O^- + Ar\left(^4P\right) \rightarrow Ar + O + e$	3×10^{-10}	t
1001	$O^- + Ar_2^* \rightarrow Ar + Ar + O + e$	3×10^{-10}	ab
1002	$O_2^- + H \rightarrow HO_2 + e$	1.5×10^{-9}	91
1003	$O_2^- + O_2 \rightarrow 2O_2 + e$	$2.7\times10^{-10}\exp(-5590/T_g)$	138
1004	$O_2^- + O_2(b) \rightarrow 2O_2 + e$	3.6×10^{-10}	93

1005	$O_2^- + O_2(a) \rightarrow 2O_2 + e$	$2\times10^{-10}(T_g/300)^{0.5}$	64
1006	$O_2^- + H_2O \rightarrow O_2 + H_2O + e$	$5\times10^{-9}\exp(-5000/T_g)$	93
1007	$O_2^- + O \rightarrow O_3 + e$	$1.5\times10^{-10}(T_g/300)^{0.5}$	64
1008	$O_2^- + Ar(^4S) \rightarrow Ar + O_2 + e$	3×10^{-10}	ab
1009	$O_2^- + Ar(^4P) \rightarrow Ar + O_2 + e$	3×10^{-10}	t
1010	$O_2^- + Ar_2^* \rightarrow 2Ar + O_2 + e$	3×10^{-10}	ab
1011	$O_2^- + Ar \rightarrow Ar + O_2 + e$	$3.9\times10^{-10}\exp(-7400/T_g)$	ab
1012	$O_3^- + Ar(^4S) \rightarrow Ar + O_2 + O + e$	1×10^{-10}	z
1013	$O_3^- + Ar(^4P) \rightarrow Ar + O_2 + O + e$	1×10^{-10}	t
1014	$O_3^- + Ar_2^* \rightarrow 2Ar + O_2 + O + e$	1×10^{-10}	z
1015	$OH^- + H \rightarrow H_2O + e$	1.8×10^{-9}	91
1016	$OH^- + O \rightarrow HO_2 + e$	2×10^{-10}	91
1017	$OH^- + Ar \rightarrow Ar + OH + e$	$2\times10^{-9}\exp(-24030/T_g)$	ab
1018	$OH^- + Ar(^4S) \rightarrow Ar + OH + e$	1×10^{-10}	z
1019	$OH^- + Ar(^4P) \rightarrow Ar + OH + e$	1×10^{-10}	t
1020	$OH^- + Ar_2^* \rightarrow 2Ar + OH + e$	1×10^{-10}	z
1021	$O_4^- + Ar(^4S) \rightarrow 2O_2 + Ar + e$	1×10^{-10}	ab
1022	$O_4^- + Ar(^4P) \rightarrow 2O_2 + Ar + e$	1×10^{-10}	t
1023	$O_4^- + Ar_2^* \rightarrow 2O_2 + 2Ar + e$	1×10^{-10}	ab
1024	$O_4^- + O(^1D) \rightarrow O + 2O_2 + e$	1×10^{-10}	120
1025	$O_4^- + O(^1S) \rightarrow O + 2O_2 + e$	1×10^{-10}	120
1026	$H_2O_3^- + Ar(^4S) \rightarrow Ar + H_2O + O_2 + e$	1×10^{-10}	ab
1027	$H_2O_3^- + Ar(^4P) \rightarrow Ar + H_2O + O_2 + e$	1×10^{-10}	t
1028	$H_2O_3^- + Ar_2^* \rightarrow 2Ar + H_2O + O_2 + e$	1×10^{-10}	ab
1029	$H_2O_3^- + H \rightarrow HO_2 + H_2O + e$	8×10^{-10}	129
1030	$H_2O_3^- + O_2(b) \rightarrow 2O_2 + H_2O + e$	1×10^{-10}	120
1031	$H_2O_3^- + O(^1D) \rightarrow O_2 + O + H_2O + e$	1×10^{-10}	120
1032	$H_2O_3^- + O(^1S) \rightarrow O_2 + O + H_2O + e$	1×10^{-10}	120
1033	$H_2O_4^- + Ar(^4S) \rightarrow Ar + H_2O + O_3 + e$	1×10^{-10}	120

1034	$H_2O_4^- + Ar\left(^4P\right) \rightarrow Ar + H_2O + O_3 + e$	1×10^{-10}	t
1035	$H_2O_4^- + Ar_2^* \rightarrow 2Ar + H_2O + O_3 + e$	1×10^{-10}	120
1036	$H_2O_2^- + Ar\left(^4S\right) \rightarrow Ar + H_2O + O + e$	1×10^{-10}	z
1037	$H_2O_2^- + Ar\left(^4P\right) \rightarrow Ar + H_2O + O + e$	1×10^{-10}	t
1038	$H_2O_2^- + Ar_2^* \rightarrow 2Ar + H_2O + O + e$	1×10^{-10}	z
1039	$H_3O_2^- + Ar\left(^4S\right) \rightarrow Ar + H_2O + OH + e$	1×10^{-10}	z
1040	$H_3O_2^- + Ar\left(^4P\right) \rightarrow Ar + H_2O + OH + e$	1×10^{-10}	t
1041	$H_3O_2^- + Ar_2^* \rightarrow 2Ar + H_2O + OH + e$	1×10^{-10}	z
1042	$H_5O_3^- + H \rightarrow 3H_2O + e$	3×10^{-10}	139
1043	$H_5O_3^- + Ar\left(^4S\right) \rightarrow Ar + 2H_2O + OH + e$	1×10^{-10}	z
1044	$H_5O_3^- + Ar\left(^4P\right) \rightarrow Ar + 2H_2O + OH + e$	1×10^{-10}	t
1045	$H_5O_3^- + Ar_2^* \rightarrow 2Ar + 2H_2O + OH + e$	1×10^{-10}	z
1046	$H_4O_4^- + H \rightarrow 2H_2O + HO_2 + e$	3×10^{-10}	139
1047	$H_4O_4^- + Ar\left(^4S\right) \rightarrow Ar + 2H_2O + O_2 + e$	1×10^{-10}	z
1048	$H_4O_4^- + Ar\left(^4P\right) \rightarrow Ar + 2H_2O + O_2 + e$	1×10^{-10}	t
1049	$H_4O_4^- + Ar_2^* \rightarrow 2Ar + 2H_2O + O_2 + e$	1×10^{-10}	z
1050	$H_6O_5^- + Ar\left(^4S\right) \rightarrow Ar + 3H_2O + O_2 + e$	1×10^{-10}	z
1051	$H_6O_5^- + Ar\left(^4P\right) \rightarrow Ar + 3H_2O + O_2 + e$	1×10^{-10}	t
1052	$H_6O_5^- + Ar_2^* \rightarrow 2Ar + 3H_2O + O_2 + e$	1×10^{-10}	z
1053	$H_4O_5^- + Ar\left(^4S\right) \rightarrow Ar + 2H_2O + O_3 + e$	1×10^{-10}	z
1054	$H_4O_5^- + Ar\left(^4P\right) \rightarrow Ar + 2H_2O + O_3 + e$	1×10^{-10}	t
1055	$H_4O_5^- + Ar_2^* \rightarrow 2Ar + 2H_2O + O_3 + e$	1×10^{-10}	z
Collisional relaxation			
1056	$O\left(^1D\right) + Ar \rightarrow O + Ar$	5×10^{-13}	140
1057	$O\left(^1D\right) + O \rightarrow 2O$	8×10^{-12}	64
1058	$O\left(^1D\right) + O_2 \rightarrow O + O_2$	$4.8\times10^{-12}\exp(67/T_g)$	64
1059	$O\left(^1D\right) + H_2O \rightarrow O + H_2O$	1.2×10^{-11}	141
1060	$O\left(^1D\right) + H \rightarrow OH$	$4.36\times10^{-32}(T_g/300)^{-1}$	u
1061	$O\left(^1D\right) + H_2 \rightarrow OH + H$	1.1×10^{-10}	93

1062	$O\left(^1D\right)+H_2O\rightarrow 2OH$	$1.62\times10^{-10}\exp(64.95/T_g)$	169
1063	$O\left(^1D\right)+H_2O\rightarrow H_2+O_2$	2.2×10^{-12}	141
1064	$O\left(^1D\right)+O_3\rightarrow 2O_2$	1.2×10^{-10}	169
1065	$O\left(^1D\right)+O_3\rightarrow 2O+O_2$	1.2×10^{-10}	169
1066	$O\left(^1D\right)+HO_2\rightarrow OH+O_2$	$2.9\times10^{-11}\exp(200/T_g)$	v
1067	$O\left(^1D\right)+H_2O_2\rightarrow H_2O+O_2$	5.2×10^{-10}	93
1068	$O\left(^1D\right)+OH\rightarrow H+O_2$	$2.1\times10^{-11}(T_g/300)^{-0.186}\exp(-153.9/T_g)$	W
1069	$O\left(^1S\right)+OH\rightarrow H+O_2$	$2.1\times10^{-11}(T_g/300)^{-0.186}\exp(-153.9/T_g)$	w
1070	$O\left(^1S\right)+O\rightarrow O\left(^1D\right)+O$	$5\times10^{-11}\exp(-301/T_g)$	93
1071	$O\left(^1S\right)+O\rightarrow 2O$	$3.33\times10^{-11}\exp(-300/T_g)$	64
1072	$O\left(^1S\right)+O_2\rightarrow O+O_2$	$4.3\times10^{-12}\exp(-850/T_g)$	93
1073	$O\left(^1S\right)+O_2\rightarrow O\left(^1D\right)+O_2$	$3.2\times10^{-12}\exp(-850/T_g)$	64
1074	$O\left(^1S\right)+H_2O\rightarrow O\left(^1D\right)+H_2O$	1.5×10^{-10}	50
1075	$O\left(^1S\right)+H_2O\rightarrow O+H_2O$	4.5×10^{-11}	50
1076	$O\left(^1S\right)+Ar\rightarrow O\left(^1D\right)+Ar$	5×10^{-17}	142
1077	$O\left(^1S\right)+H_2\rightarrow OH+H$	2.6×10^{-16}	143
1078	$O\left(^1S\right)+H\rightarrow OH$	$4.36\times10^{-32}(T_g/300)^{-1}$	u
1079	$O\left(^1S\right)+O_3\rightarrow 2O_2$	4.63×10^{-10}	169
1080	$O\left(^1S\right)+H_2O\rightarrow 2OH$	3×10^{-10}	50
1081	$O\left(^1S\right)+H_2O\rightarrow H_2+O_2$	2.2×10^{-12}	50
1082	$O\left(^1S\right)+HO_2\rightarrow OH+O_2$	$2.9\times10^{-11}\exp(200/T_g)$	v
1083	$O\left(^1S\right)+H_2O_2\rightarrow H_2O+O_2$	5.2×10^{-10}	x
1084	$O_2(a)+Ar\rightarrow Ar+O_2$	$3\times10^{-18}\exp(-200/T_g)$	30
1085	$O_2(a)+H_2\rightarrow H_2+O_2$	1.5×10^{-18}	169
1086	$O_2(a)+O\rightarrow O_2+O$	7×10^{-16}	93
1087	$O_2(a)+O_2\rightarrow 2O_2$	$2.2\times10^{-18}(T_g/300)^{0.8}$	93
1088	$O_2(a)+HO_2\rightarrow HO_2+O_2$	1.66×10^{-11}	144

1089	$O_2(a) + H_2O \rightarrow H_2O + O_2$	3×10^{-18}	169
1090	$O_2(a) + H \rightarrow OH + O$	$1.83\times10^{-13}\exp(-1550/T_g)$	138
1091	$O_2(a) + O_3 \rightarrow 2O_2 + O$	$5.2\times10^{-11}\exp(-2840/T_g)$	169
1092	$O_2(a) + O_2 \rightarrow O_3 + O$	2.96×10^{-21}	169
1093	$O_2(b) + O_2 \rightarrow 2O_2$	$4\times10^{-18}(T_g/300)^{0.5}$	64
1094	$O_2(b) + O_2 \rightarrow O_2(a) + O_2$	$3.6\times10^{-17}(T_g/300)^{0.5}$	64
1095	$O_2(b) + Ar \rightarrow Ar + O_2(a)$	1×10^{-17}	145
1096	$O_2(b) + H_2 \rightarrow H_2 + O_2$	1.5×10^{-18}	y
1097	$O_2(b) + O \rightarrow O_2 + O$	$8\times10^{-15}(T_g/300)^{0.5}$	64
1098	$O_2(b) + O \rightarrow O_2(a) + O$	$7.2\times10^{-14}(T_g/300)^{0.5}$	64
1099	$O_2(b) + HO_2 \rightarrow HO_2 + O_2$	1.66×10^{-11}	o
1100	$O_2(b) + H_2O \rightarrow H_2O + O_2$	3×10^{-18}	93
1101	$O_2(b) + H_2O \rightarrow H_2O + O_2(a)$	$4.52\times10^{-12}\exp(89/T_g)$	51
1102	$O_2(b) + O_3 \rightarrow O_2(a) + O_3$	$7.33\times10^{-12}(T_g/300)^{0.5}$	64
1103	$O_2(b) + O_3 \rightarrow O_2 + O_3$	$7.33\times10^{-12}(T_g/300)^{0.5}$	64
1104	$O_2(b) + O_3 \rightarrow 2O_2 + O$	$7.33\times10^{-12}(T_g/300)^{0.5}$	64
1105	$O_2(b) + H \rightarrow OH + O$	$1.83\times10^{-13}\exp(-1550/T_g)$	c
1106	$OH(A) + Ar \rightarrow Ar + OH$	1×10^{-13}	146
1107	$OH(A) + O_2 \rightarrow O_2 + OH$	$7.5\times10^{-11}(T_g/300)^{0.5}$	147
1108	$OH(A) + H_2O \rightarrow H_2O + OH$	$4.9\times10^{-10}(T_g/300)^{0.5}$	147
1109	$OH(A) + H \rightarrow H_2 + O$	$5.8\times10^{-10}(T_g/300)^{0.5}$	147
1110	$OH(A) + H \rightarrow H_2O$	$6.87\times10^{-31}(T_g/300)^{-2}$	g
1111	$OH(A) + O \rightarrow H + O_2$	$4.3\times10^{-11}(T_g/300)^{0.5}$	147
1112	$OH(A) + H_2 \rightarrow H + H_2O$	$1.3\times10^{-10}(T_g/300)^{0.5}$	147
1113	$OH(A) + OH \rightarrow H_2O + O$	$1.65\times10^{-12}(T_g/300)^{1.14}\exp(-50.03/T_g)$	h
1114	$OH(A) + OH \rightarrow H_2O_2$	$1.5\times10^{-11}(T_g/300)^{-0.37}$	148
1115	$OH(A) + H_2O_2 \rightarrow H_2O + HO_2$	2.93×10^{-10}	149
1116	$Ar_2^* + M \rightarrow 2Ar + M$	1.5×10^{-15}	ab
1117	$Ar_2^* + H_2 \rightarrow 2H + 2Ar$	6×10^{-11}	m
1118	$Ar_2^* + O_2 \rightarrow 2O + 2Ar$	5.8×10^{-11}	n
1119	$Ar_2^* + H_2O \rightarrow 2Ar + H + OH$	1.4×10^{-9}	150
1120	$Ar_2^* + H_2O_2 \rightarrow 2OH + 2Ar$	4.5×10^{-10}	150

1121	$Ar_2^* + OH \rightarrow Ar + Ar + O + H$	6.6×10^{-11}	30
1122	$Ar_2^* + O_3 \rightarrow O_2 + O + 2Ar$	5.8×10^{-11}	p
1123	$Ar\left(^4S\right) + O_2 \rightarrow O_2 + Ar$	1.12×10^{-9}	151
1124	$Ar\left(^4S\right) + H_2 \rightarrow Ar + 2H$	6×10^{-11}	152
1125	$Ar\left(^4S\right) + O_2 \rightarrow 2O + Ar$	5.8×10^{-11}	153
1126	$Ar\left(^4S\right) + O_3 \rightarrow O_2 + O + Ar$	5.8×10^{-11}	118
1127	$Ar\left(^4S\right) + H_2O \rightarrow Ar + OH + H$	3.312×10^{-10}	154
1128	$Ar\left(^4S\right) + H_2O_2 \rightarrow Ar + 2OH$	3.312×10^{-10}	l
1129	$Ar\left(^4S\right) + Ar \rightarrow 2Ar$	2.09×10^{-15}	155
1130	$Ar\left(^4P\right) + 2Ar \rightarrow Ar + Ar_2^*$	1.2×10^{-32}	145
1131	$Ar\left(^4P\right) + Ar \rightarrow 2Ar$	1×10^{-11}	156
1132	$Ar\left(^4P\right) + O_2 \rightarrow Ar + 2O$	2.96×10^{-10}	157
1133	$Ar\left(^4P\right) + H_2 \rightarrow Ar + 2H$	6×10^{-11}	168
1134	$Ar\left(^4P\right) + H_2O_2 \rightarrow 2OH + Ar$	4.5×10^{-10}	168
1135	$Ar\left(^4P\right) + H_2O \rightarrow OH + H + Ar$	3.312×10^{-10}	168
1136	$Ar\left(^4P\right) + O_3 \rightarrow Ar + O_2 + O$	5.8×10^{-11}	150
Penning ionization			
1137	$2Ar\left(^4S\right) \rightarrow Ar^+ + Ar + e$	$5\times10^{-10}(T_g/300)^{0.5}$	158
1138	$Ar\left(^4S\right) + Ar_2^* \rightarrow Ar^+ + 2Ar + e$	5×10^{-10}	ab
1139	$Ar\left(^4S\right) + Ar_2^* \rightarrow Ar_2^+ + Ar + e$	$7\times10^{-10}(T_g/300)^{0.5}$	85
1140	$2Ar_2^* \rightarrow Ar_2^+ + 2Ar + e$	$7\times10^{-10}(T_g/300)^{0.5}$	85
1141	$Ar\left(^4P\right) + Ar_2^* \rightarrow Ar_2^+ + Ar + e$	5×10^{-10}	30
1142	$Ar\left(^4P\right) + Ar_2^* \rightarrow Ar^+ + Ar + Ar + e$	5×10^{-10}	30
1143	$Ar\left(^4P\right) + Ar\left(^4S\right) \rightarrow Ar + + Ar + e$	5×10^{-10}	30
1144	$2Ar\left(^4P\right) \rightarrow Ar^+ + Ar + e$	5×10^{-10}	159
Radiation			
1145	$O\left(^1D\right) \rightarrow O + h\nu$	5×10^{-3}	93
1146	$O\left(^1S\right) \rightarrow O\left(^1D\right) + h\nu$	1.34	93
1147	$O_2(a) \rightarrow O_2 + h\nu$	2.7×10^{-4}	160

1148	$O_2(b) \rightarrow O_2 + h\nu$	8.3×10^{-2}	161
1149	$OH(A) \rightarrow OH + h\nu$	1.25×10^{6}	162
1150	$Ar_2^* \rightarrow 2Ar + h\nu$	3.5×10^{5}	163
1151	$Ar(^4P) \rightarrow Ar + h\nu$	3.2×10^{7}	164
Others reactions for neutral species			
1152	$Ar + 2H \rightarrow Ar + H_2$	$6.04\times10^{-33}(T_g/300)^{-1}$	q
1153	$Ar + H + O \rightarrow Ar + OH$	$3.2\times10^{-33}(T_g/300)^{-1}$	ab
1154	$Ar + H + O_2 \rightarrow Ar + HO_2$	$2\times10^{-32}(T_g/300)^{-0.8}$	ab
1155	$Ar + H + OH \rightarrow Ar + H_2O$	$1.48\times10^{-30}(T_g/300)^{-1.18}\exp(-312/T_g)$	165
1156	$Ar + 2O \rightarrow Ar + O_2$	$4.5\times10^{-34}\exp(630/T_g)$	166
1157	$Ar + 2O \rightarrow Ar + O_2(a)$	9.88×10^{-35}	ab
1158	$Ar(^4S) + 2Ar \rightarrow Ar_2^* + Ar$	1.1×10^{-32}	118
1159	$Ar(^4S) + H_2O \rightarrow Ar + H + OH(A)$	1.488×10^{-10}	167
1160	$Ar(^4P) + O_2 \rightarrow Ar + O + O(^1D)$	3.34×10^{-10}	168
1161	$Ar(^4P) + H_2O \rightarrow OH(A) + H + Ar$	1×10^{-10}	168
1162	$Ar_2^* + M \rightarrow Ar(^4S) + Ar + M$	2×10^{-14}	30
1163	$2H \rightarrow H_2$	$6.04\times10^{-33}(T_g/300)^{-1}$	169
1164	$H + O \rightarrow OH$	$4.36\times10^{-32}(T_g/300)^{-1}$	169
1165	$H + O_2 \rightarrow OH + O$	$1.62\times10^{-10}\exp(-7470/T_g)$	169
1166	$H + O_2 \rightarrow HO_2$	$5.4\times10^{-32}(T_g/300)^{-1.8}$	169
1167	$H + OH \rightarrow H_2 + O$	$6.86\times10^{-14}(T_g/300)^{2.8}\exp(-1950/T_g)$	169
1168	$H + OH \rightarrow H_2O$	$6.87\times10^{-31}(T_g/300)^{-2}$	169
1169	$H + HO_2 \rightarrow H_2O + O$	$9.18\times10^{-11}\exp(-971.9/T_g)$	93
1170	$H + HO_2 \rightarrow H_2O + O(^1D)$	$3.29\times10^{-12}(T_g/300)^{1.55}\exp(80.58/T_g)$	169
1171	$H + HO_2 \rightarrow H_2 + O_2$	$2.57\times10^{-11}(T_g/300)^{0.5598}\exp(-346/T_g)$	93
1172	$H + HO_2 \rightarrow H_2 + O_2(a)$	$2.96\times10^{-12}(T_g/300)^{1.63}\exp(-2000/T_g)$	169
1173	$H + HO_2 \rightarrow 2OH$	$2.35\times10^{-10}\exp(-373.7/T_g)$	93
1174	$H + H_2O_2 \rightarrow H_2 + HO_2$	$8\times10^{-11}\exp(-4000/T_g)$	93
1175	$H + H_2O_2 \rightarrow H_2O + OH$	$4\times10^{-11}\exp(-2000/T_g)$	93
1176	$H + H_2O \rightarrow H_2 + OH$	$6.82\times10^{-12}(T_g/300)^{1.6}\exp(-9720/T_g)$	169
1177	$H + O_3 \rightarrow OH + O_2$	$2.72\times10^{-11}(T_g/300)^{0.75}$	169

1178	$H + O_3 \rightarrow O + HO_2$	7.51×10^{-13}	169
1179	$H_2 + O \rightarrow OH + H$	$9\times10^{-12}(T_g/300)^{1}\exp(-4480/T_g)$	93
1180	$H_2 + OH \rightarrow H + H_2O$	$2.31\times10^{-12}(T_g/300)^{1.47}\exp(-1761/T_g)$	93
1181	$H_2 + HO_2 \rightarrow H_2O_2 + H$	$5\times10^{-11}\exp(-13110/T_g)$	169
1182	$H_2 + H_2O \rightarrow OH + H + H_2$	$5.8\times10^{-9}\exp(-52900/T_g)$	87
1183	$2O \rightarrow O_2$	$9.26\times10^{-34}(T_g/300)^{-1}$	169
1184	$O + OH \rightarrow H + O_2$	$2.1\times10^{-11}(T_g/300)^{-0.186}\exp(-153.9/T_g)$	93
1185	$O + HO_2 \rightarrow OH + O_2$	$2.9\times10^{-11}\exp(200/T_g)$	93
1186	$O + H_2O_2 \rightarrow OH + HO_2$	$1.79\times10^{-13}(T_g/300)^{2.92}\exp(-1294/T_g)$	93
1187	$O + H_2O \rightarrow 2OH$	$1.66\times10^{-11}(T_g/300)^{1.14}\exp(-8624/T_g)$	138
1188	$O + H_2O \rightarrow HO_2 + H$	1.86×10^{-62}	169
1189	$O + H_2O \rightarrow O_2 + H_2$	1.86×10^{-62}	169
1190	$O + O_3 \rightarrow 2O_2$	$8\times10^{-12}\exp(-2060/T_g)$	169
1191	$O_2 + O\left(^1D\right) \rightarrow O + O_2\left(b\right)$	$2.56\times10^{-11}\exp(67/T_g)$	64,93
1192	$O_2 + O\left(^1D\right) \rightarrow O + O_2\left(a\right)$	$1.6\times10^{-12}\exp(67/T_g)$	64
1193	$O_2 + H_2O_2 \rightarrow 2HO_2$	$9\times10^{-11}\exp(-19965/T_g)$	169
1194	$O_2 + H_2O \rightarrow HO_2 + OH$	$7.72\times10^{-12}\exp(-37284/T_g)$	169
1195	$O_3 + M \rightarrow O_2 + O + M$	$1.56\times10^{-9}\exp(-11490/T_g)$	64
1196	$2OH \rightarrow H_2O + O$	$1.65\times10^{-12}(T_g/300)^{1.14}\exp(-50.03/T_g)$	169
1197	$OH + HO_2 \rightarrow O_2 + H_2O$	$4.38\times10^{-11}\exp(110.9/T_g)$	93
1198	$OH + H_2O_2 \rightarrow H_2O + HO_2$	$4.53\times10^{-12}\exp(-288.9/T_g)$	93
1199	$OH + O_3 \rightarrow HO_2 + O_2$	$1.69\times10^{-12}\exp(-941/T_g)$	169
1200	$HO_2 \rightarrow H + O_2$	$2.41\times10^{-8}(T_g/300)^{-1.18}\exp(-24415/T_g)$	169
1201	$HO_2 + H_2O \rightarrow H_2O_2 + OH$	$4.65\times10^{-11}\exp(-16477/T_g)$	169
1202	$HO_2 + O_3 \rightarrow OH + 2O_2$	$1.97\times10^{-16}(T_g/300)^{4.57}\exp(693/T_g)$	169
1203	$H_2O_2 \rightarrow 2OH$	$2.03\times10^{-3}(T_g/300)^{-4.86}\exp(-26821/T_g)$	169
1204	$3H \rightarrow H + H_2$	$6\times10^{-31}(T_g/300)^{-1}$	104
1205	$2H + H_2 \rightarrow 2H_2$	$8.1\times10^{-33}(T_g/300)^{-0.6}$	148
1206	$2H + H_2O \rightarrow H_2 + H_2O$	$1.32\times10^{-31}(T_g/300)^{-1.25}$	148

1207	$H + O + H_2 \rightarrow OH + H_2$	$9.19\times10^{-33}(T_g/300)^{-1}$	148
1208	$H + O + H_2O \rightarrow OH + H_2O$	$2.76\times10^{-32}(T_g/300)^{-1}$	148
1209	$H + O_2 + H_2 \rightarrow HO_2 + H_2$	$5.72\times10^{-32}(T_g/300)^{-0.86}$	148
1210	$H + O_2 + O_2 \rightarrow HO_2 + O_2$	$5.72\times10^{-32}(T_g/300)^{-0.86}$	148
1211	$H + O_2 + H_2O \rightarrow HO_2 + H_2O$	$4.08\times10^{-31}(T_g/300)^{-0.76}$	148
1212	$H + OH + H_2 \rightarrow H_2O + H_2$	$4.92\times10^{-31}(T_g/300)^{-2}$	148
1213	$H + OH + O_2 \rightarrow H_2O + O_2$	$6.74\times10^{-31}(T_g/300)^{-2}$	148
1214	$H + OH + H_2O \rightarrow 2H_2O$	$2.46\times10^{-30}(T_g/300)^{-2}$	148
1215	$3O \rightarrow O + O_2$	$9.21\times10^{-34}(T_g/300)^{-0.63}$	64
1216	$2O + O_2 \rightarrow O_3 + O$	$3.4\times10^{-34}\exp(345/T_g)$	170
1217	$O + 2O_2 \rightarrow O_3 + O_2$	$6\times10^{-34}(T_g/300)^{-2.8}$	64
1218	$O + O_2 + M \rightarrow O_3 + M$	$3.4\times10^{-34}\exp(510/T_g)$	171
1219	$3O \rightarrow O + O_2(a)$	$6.93\times10^{-35}(T_g/300)^{-0.63}$	64
1220	$2O + H_2 \rightarrow H_2 + O_2$	$2.65\times10^{-33}(T_g/300)^{-1}$	148
1221	$2O + O_2 \rightarrow 2O_2$	$2.65\times10^{-33}(T_g/300)^{-0.63}$	64
1222	$2O + O_2 \rightarrow O_2 + O_2(a)$	$1.93\times10^{-35}(T_g/300)^{-0.63}$	64
1223	$2O + H_2O \rightarrow H_2O + O_2$	$1.7\times10^{-32}(T_g/300)^{-1}$	148
1224	$2OH + H_2O_2 \rightarrow 2H_2O_2$	$7.48\times10^{-32}(T_g/300)^{-0.9}\exp(856/T_g)$	148
1225	$2OH + O_2 \rightarrow O_2 + H_2O_2$	$6.05\times10^{-31}(T_g/300)^{-3}$	93
1226	$2OH + H_2O \rightarrow H_2O + H_2O_2$	$1.54\times10^{-31}(T_g/300)^{-2.021}\exp(183.6/T_g)$	93
1227	$2OH + Ar \rightarrow H_2O_2 + Ar$	$6.12\times10^{-31}(T_g/300)^{-3.2}$	172
1228	$2HO_2 + Ar \rightarrow H_2O_2 + O_2 + Ar$	3.69×10^{-32}	173

[a] $f(T_e)$ indicates that the rate coefficient is obtained from EEDF using cross section from indicated reference.

[b] Rate coefficients have units of $cm^3\ s^{-1}$ for two-body reactions and $cm^6\ s^{-1}$ for three-body reactions; T_e has unitseV; T_g has units K.

[c] momentum transfer cross sections are not well known. Here I took elastic cross sections as the Q_{el}. In ref.1 the cross section data is not shown for Te<50eV, I assumed in that range the cross sections are equal to that of 50eV.

[d] Cross section estimated by shifting and scaling the ground state cross section by the excitation threshold.

[e] Estimated same as O_4^+

[f] M isEstimated same as O_2

[g] Estimated same as $OH+H \rightarrow H_2O$

[h] Estimated same as $OH+OH \rightarrow H_2O+O$

[i] Estimated same as $2e+H_5O_2^+ \rightarrow 2H_2O+H+e$

[j] Estimated same as $O_2(a)+H \rightarrow OH+O$

[k] These two cross sections are not well known. Here I took $(Q_{inel}-Q_i)/2$ as their cross sections.

[l] Estimated same as $Ar(^4S)+H_2O \rightarrow Ar+OH+H$

[m] Estimated same as $Ar(^4S)+H_2 \rightarrow Ar+2H$

[n] Estimated same as $Ar(^4S)+O_2 \rightarrow 2O+Ar$

[o] Estimated same as $O_2(a)+HO_2 \rightarrow HO_2+O_2$

[p] Estimated same as $Ar(^4S)+O_3 \rightarrow O_2+O+Ar$

[q]Estimated same as $2H \rightarrow H_2$
[r]Estimated same as $e+O_2+H_2O \rightarrow O_2^- + H_2O$
[s]Estimated same as $e+O_2+Ar \rightarrow O_2^- + Ar$
[t]Collisional detachment $Ar(^4P)$ coefficient based on $Ar(^4S)$
[u]Estimated same as $H+O \rightarrow OH$
[v]Estimated same as $O+HO_2 \rightarrow OH+O_2$
[w]Estimated same as $O+OH \rightarrow H+O_2$
[x]Estimated same as $O(^1D)+H_2O_2 \rightarrow H_2O+O_2$
[y]Estimated same as $O_2(a)+H_2 \rightarrow H_2+O_2$
[z]Estimated same as$H^- + OH \rightarrow H_2O + e$
[ab]Estimated same as He

Reference

[1]Hackam R and Akiyama H 2000 *IEEE Trans. Dielec. Elec. Insul.***7** 654

[2]Malik M A, Chaffar A and Malik S A 2001 *Plasma Sources Sci. Technol.***10** 82-91

[3]Olszewski P, Li J F, Liu D X and Walsh J L 2014 *J. Haz. Mat.***279** 60-66

[4]Gonzalez II E, Barankin M D, Guschl P C and Hicks R F 2010 *Plasma Process.Polym.***7** 482-93

[5]Bhoj A N and Kushner M J 2008 *Plasma Sources Sci. Technol.***17** 035024

[6] Shao T, Zhang C, Long K H, Zhang D D, Jue W, Yan P and Zhou Y X 2010 *Appl. Surf. Sci.***256** 3888-94

[7] Kong M G, Kroesen G, Morfill G, Nosenko T, Shimizu T, Dijk J V and Zimmermann J L 2009 *New J. Phys.* **11** 115012

[8]Zhong S Y, Dong Y Y, Liu D X, Xu D H, Xiao S X, Chen H L and Kong M J 2016 *British J. Dermatology***174** 542-52

[9]Xu D H, Liu D X, Wang B Q, Chen C, Chen Z Y, Li D, Yang Y J, Chen H L and Kong M G 2015 *Plos One***10** e0128205

[10] Samukawa S *et al* 2012 *J. Phys. D: Appl. Phys.***45** 253001

[11]Graves D B 2012 *J. Phys. D: Appl. Phys.***45** 263001

[12]Fleischman M S, Lee B S, Rodriguez-Santiago V, Chhasatia V, Sun Y, Pappas D D 2012*Surf.Coat. Technol.***206** 3923-30

[13]Chen J H and Wang P X 2005 *IEEE Trans. Plasma Sci.***33** 808-812

[14] Rodriguez-Santiago V, Bujanda A A, Stein B E and Pappas D D 2011 *Plasma Process. Polym.***8** 631-9

[15]Vasko C A, Liu D X, van Veldhuizen E M, Iza F and Bruggeman P J 2014 *Plasma Chem. Plasma Process.***34** 1081-99

[16] Srivastava N and Wang C J 2011 *J. Appl. Phys.***110** 053304

[17]Dodet B, Odic E, Goldman A, Goldman M and Renard D 2005*J. Adv. Oxid.* Technol. **8** 91-97

[18] Nikiforov A Y, Saraniand A and Leys C 2011 *Plasma Sources Sci. Technol.***20** 015014

[19]Yonemori S, Nakagawa Y, Ono R and Oda T 2012 *J. Phys. D: Appl. Phys.***45** 225202

[20]Perry R H and Green D W 1997 *Perry's Chemical Engineers' Handbook* 7th edn (New York: McGraw-Hill)

[21]Bruggeman P and Leys C 2009 *J. Phys. D: Appl. Phys.***42** 053001

[22]Liu D X, Bruggeman P, Iza F, Rong M Z and Kong M G 2010 *Plasma Sources Sci. Technol.***19** 025018

[23]Mckay K, Liu D X, Rong M Z, Iza F and Kong M G 2011 *Appl. Phys. Lett.***99** 091501

[24]Mckay K, Liu D X, Rong M Z, Iza F and Kong M G 2012 *J. Phys. D: Appl. Phys.***45** 172001

[25]Tian W and Kushner M J 2014 *J. Phys. D: Appl. Phys.***47** 165201

[26]Dorai R and Kushner M J 2003 *J. Phys. D: Appl. Phys.***36** 666

[27] Park G, Lee H, Kim G and Lee J K 2008 *Plasma Process. Polym.***5** 569

[28]Murakami T, Niemi K and Gans T2013 *Plasma Sources Sci. Technol.***22** 015003

[29]Liu D X, Iza F, Wang X H, Kong M G and Rong M Z 2011 *Appl. Phys. Lett.***98** 221501

[30]van Gaens W and Bogaerts A 2013 *J. Phys. D: Appl. Phys.***46** 275201

[31] http://www.tis-gdv.de/tis/misc/klima.htm

[32]Bruggeman P, Iza F, Lauwers D and Gonzalvo Y A 2010 *J. Phys. D: Appl. Phys.***43** 012003

[33]Kushner M J 1999 *Bull. Am. Phys. Soc.***44** 63

[34]Hagelaar G J M and Pitchford L C 2005 *Plasma Sources Sci. Technol.***14** 722

[35] Liu D X, Rong M Z, Wang X H, Iza F, Kong M G and Bruggeman P 2010 *Plasma Process. Polym.***7** 846-865

[36] Ding K, Lieberman M A and Lictenberg A J 2014 *J. Phys. D: Appl. Phys.* **47** 305203

[37]Yang A J, Wang X H, Rong M Z, Liu D X, Iza F and Kong M G 2011 *Phys. Plasmas***18** 113503

[38]Lieberman M A and Lichtenberg A J 2002 *Principles of Plasma Discharges and Materials Processing 2nd edn* (New York: Wiley) p 173.

[39]Perin J, Leroy O and Bordage M C 1996 *Contrib. Plasma Phys.***36** 3

[40]Liu D X, Iza F, Wang X H, Ma Z Z, Rong M Z and Kong M G 2013 *Plasma Sources Sci. Technol.***22** 055016

[41] Monahan D D and Turner M M 2008 *Plasma Sources Sci. Technol.***17** 045003

[42]Liu D X, LiJ F, Yang A J, Wang X H, Rong M Z and Kong M G 2016 *High Voltage* **1** 81-85

[43]Chen C, Liu D X, Liu Z C, Yang A J, Chen H L, Shama G and Kong M G 2014 *Plasma Chem. Plasma Process.* **34** 403-41

[44] Lindsay A, Anderson C, Slikboer E, Shannon S and Graves D 2015 *J. Phys. D: Appl. Phys.* **48** 424007

[45] Bruggeman P J et al. 2016 *Plasma Sources Sci. Technol.***25** 53002

[46]Yagi I, Ono R, Oda T and Takaki K 2015 *Plasma Sources Sci. Technol.***24** 015002

[47]Yang A J, Liu D X, Rong M Z, Wang X H and Kong M G 2014 *Phys. Plasmas***21** 083501

[48]Yang A J, Rong M Z, Wang X H, Liu D X and Kong M G 2013 *J. Phys. D: Appl. Phys.***46** 415201

[49]Liu D X, Yang A J, Wang X H, Rong M Z, Iza F and Kong M G 2012 *J. Phys. D: Appl. Phys.***45** 305205

[50] Slanger T G and Black G 1978 *J. Chem. Phys.***68** 989-97

[51] Dunlea E J, Talukdar R K and Ravishankara A R 2005 *J. Phys. Chem. A***109** 3912-20

[52] Motret O, Hibert C, Pellerin S and Pouvesle J M 2000 *J. Phys. D: Appl. Phys.***33** 1493-8

[53] Sarani A, Nikiforov A Y and Leys C 2010 *Phys. Plasmas***17** 063504

[54]Dilecce G and Benedictis S D 2011 *Plasma Phys. Control. Fusion***53** 124006

[55]Kirkpatrick M J 2007*Int. J.plasma Environ.sci. thechnol.***1** 96-101

[56] http://www.who.int/mediacentre/factsheets/fs313/en/

[57] Ding K and Lieberman M A 2015 *J. Phys. D: Appl. Phys.***48** 035401

[58] Phelps A ftp://jila.colorado.edu/collision data

[59] Itikawa Y and Mason N 2005 *J. Phys. Chem. Ref. Data***34** 1-22

[60]Phelps A V1985 *JILA Information Center Report* No 28

[61] Itikawa Y, Ichimura A, Onda K, Sakimoto K, Takayanagi K, Hatano Y, Hayashi M, Nishimura H and TsurubuchiS 1989 *J. Phys. Chem. Ref. Data* **18** 23

[62] Joshipuru K N, Vinodkumar M and Patel U M 2001 *J. Phys. B:At. Mol. Opt. Phys.***4** 509

[63] Janev R K, Langer W D, Evans J K and Post D E 1987 *Elementary processes in hydrogen-helium plasmas*(Berlin: Springer)

[64] Stafford D S and Kushner M J 2004 *J. Appl. Phys***96** 2451-65

[65] Riahi R, Teulet P, Lakhdar Z B and Gleizes A 2006 *Eur. Phys. J. D***40** 223-30

[66] Soloshenko I A, Tsiolko V V, Khomich V A 2002 *IEEE Trans. Plasma Sci.***30** 1440-44

[67]Steinfeld J I, Adler-Golden S M and Gallagher J W 1987 *J. Phys. Chem. Ref. Data***16** 911

[68] Rapp D and Englander-Golden P 1965 *J. Chem. Phys.* **43** 1464

[69] Vriens L 1964 *Phys. Lett.***8** 260-1

[70] McCann K J and Flannery M R 1979 *Appl. Phys. Lett.***34** 1

[71] Tawara H, Itikawa Y, Nishimura H and Youshino M 1990 *J. Phys. Chem. Ref. Data***19** 617-36

[72] Laher R R and Gilmore F R 1990 *J. Phys. Chem. Ref. Data***19** 277-305

[73]Eliasson B and Kogelschatz U 1986*Basic data for modelling of electrical discharges in gases: oxygen*(ABB Asea Brown Boveri).

[74]McConkey J W, Malone C P, Johnson P V, Winstead C, McKoy V and Kanik I 2008 *Phys. Rep.***466** 1

[75]Ionin A A, Kochetov I V, Napartovich A P and Yuryshev N N 2007 *J. Phys. D: Appl. Phys.***40** R25-R61

[76]BOLSIG+ software version 1.1. 2008 http://www.siglo-kinema.com/technical.htm (accessed April, 2010)

[77]Hall R I and Trajmar S 1075 *J. Phys. B: Atom. Molec. Phys.***8** L293

[78] Gudmundsson J T, Kouznetsov I G, Patel K K and Lieberman M A 2001 *J. Phys. D: Appl. Phys.***34** 1100-09

[79] Gudmundsson J T and Thorsteinsson E G 2007 *Plasma Sources Sci. Technol.***16** 399-412

[80] Yousfi M and Benabdessadok M D 1996 *J. Appl. Phys.***80**6619

[81] Soloshenko I A, Tsiolko V V, Pogulay S S, Terentyeva A G, Bazhenov V Y, Shchedrin A I, Ryabtsev A V and Kuzmichev A I 2007 *Plasma Sources Sci. Technol.***16** 56-66

[82]Samiolovich V G, Popovich M P, Emelyanov Yu M and Filippov Yu V 1966 *J. Phys. Chem.***40** 287

[83] Petrov G M, Giuliani J L and Dasgupta A 2002 *J. Appl. Phys.* **91** 2662

[84]Gottscho R A, Scheller G R, Intrator T and Graves D B 1988 *J. Vac. Sci. Technol.*A **6** 1393

[85]Ashida S, Lee C and Lieberman M A 1995 *J. Vac. Sci. Technol.*A **13** 2498

[86] Neeser S, Kunz T and Langhoff H 1997 *J. Phys. D: Appl. Phys.***30** 1489

[87]Millar T J, Farquhar P R A and Willacy K 1997 *Astron. Astrophys. Suppl. Ser.***121** 139-85

[88]Tawara H, Itikawa Y, Nishimura H and Yoshino M 1990 *J. Phys. Chem. Ref. Data***19** 617-36

[89]Itikawa Y and Ichimura A 1990 *J. Phys. Chem. Ref. Data***19** 637

[90]Burrow P D 1973 *J. Chem. Phys.***59** 4922

[91] McEwan M J and Phillips L F 1975 *Chemistry of the Atmosphere* (London: Edward Arnold)

[92]Nandi D, Krishnakumar E, Rosa A, Schmidt W F and Illenberger E 2003 *Chem. Phys. Lett.***373** 454-9

[93] Gordillo-V ázquez1 F G 2008 *J. Phys. D: Appl. Phys.***41** 234016

[94] Salabas A, Marques L, Jolly J, Gousset G and Alves L L 2004 *J. Appl. Phys.***95** 4605

[95] Rowe B R, Vallee F, Queffelec J L, Gomet J C and Morlais M 1988 *J. Chem. Phys.***88** 845-50

[96]Bortner M H and Baurer T 1978 (eds) *Defence Nuclear Agency Reaction Rate Handbook* 2nd edn, DNA 1948H (General Electric, TEMPO) ch 24

[97] Huang C M, Whitaker M, Biondi M A and Johnsen R 1978 *Phys. Rev.* A **18** 64-7

[98] Mitchell J B A 1990 *Phys. Rep.***186** 215-48

[99]Bogaerts A and Gijbels R 2000 *J. Anal.At.Spectrom.*15 441-9

[100] Bultel A, van Ootegem B, Bourdon A and Vervisch P 2002 *Phys. Rev.* E **65** 046406

[101]Bogaerts A and Gijbels R 1999*J. Appl. Phys.***86** 4124

[102] Aleksandrov N L, Konchakov A M, Shachkin L V and Shashkov V M 1986 *Sou. Plasma Phys.***12** 1218-24

[103]Niles F E 1974 Report No. 1702, US Army, Aberdeen Proving Grounds, Maryland 21005 pp 1-107.

[104] Giuliani J L, Shamamian V A, Thomas R E, Apruzese J P, Mulbrandon M, Rudder R A, Hendry R C, Robson A E 1999 *IEEE Trans. Plasma Sci.***27** 1317-28

[105] Meeks E, Larson R S, Ho P, Apblett C, Han S M, Edelberg E and Aydil E S 1998 *J. Vac. Sci. Technol.* A **16** 544

[106]Scott C D and Lefebvre M 1996 *J. Thermophys.Heat. Transfer***10** 426-35

[107] Hassouni K, Grotjohn T A, Gicquel A 1999 *J. Appl. Phys.***86** 134

[108] Kossyi I A, Kostinsky A Y, Matveyev A A and Silakov V P 1992 *Plasma Sources Sci. Technol.***1** 207-20

[109] Konstantinovskii R S, Shibkov V M and Shibkova L V 2005 *Kinetics and Catalysis***46** 775-88

[110]Smith R D, Smith D L and Futrell J H 1976 *Int. J. Mass Spectrom. Ion Phys.***19** 395

[111]Gaucherel P and Rowe B 1977 *Int. J. Mass Spectrom. Ion Phys.***25** 211

[112] Midey A J and Viggiano A A 1998 *J. Chem. Phys.***109** 5257

[113] Karpas Z, Anicich V G and Huntress W T 1978 *Jr. Chem. Phys. Lett.***59** 84

[114] Bolder R C and Twiddy N D 1972 *Faraday Discuss. Chem. Soc.* **53** 192

[115] Shul R J, Upschulte B L, Passarella R, Keesee R G and Castleman A W 1987 *J. Phys. Chem.* **91** 2256-62

[116] Bohme D K, Adams N G, Mosesman M, Dunkin D B and Ferguson E E 1970 *J. Chem. Phys.***52** 5094

[117] Fehsenfeld F C, Schmeltekopf A L and Ferguson E E 1967 *J. Chem. Phys.***46** 2802-8

[118] Ferreira C M and Loureiro J 1983 *J. Phys. D: Appl. Phys.***16** 1611

[119] Anicich V G 1993 *J. Phys. Chem. Ref. Data***22** 1469-569

[120]Vidmar R J and Stalder K R 2004 Computations of the power to sustain plasma in air with relevance to aerospace technology *Final Report* AFRL-SR-AR-TR-04-0123

[121] Molina-Cuberos G J, Lopez-Moreno J J, Rodrigo R, Lichtenegger H and Schwingenschuh K 2001 *Adv. Space Res.***27** 1801-6

[122]Ferguson E E 1973 *Atomic Data Nucl. Data Tables***12** 159-78

[123] Good A 1975 *Chem. Rev.***75** 561-83

[124] Sieck L W, Herron J T and Green D S 2000 *Plasma Chem. Plasma Process.***20** 235-58

[125]Ferguson E E 1973 *Atomic Data Nucl. Tables.***12** 159-78

[126]Axford S D T and Hayhurst A N 1996 *Proc. Math. Phys. Eng. Sci.***452** 1007-33

[127]Fehsenfeld F C, Carleton J H and Ferguson E E 1973 *J. Chem. Phys.* **58** 5841-2

[128]Gravendeel B and Hoog F J D 1987 *J. Phys. B: At. Mol. Phys.***20** 6337-61

[129] Fritzenwallner J and Kopp E 1998 *Adv. Space Res.***21** 891-4

[130]Jones J D C, Lister D G, Wareing D P and Twiddy N D 1980 *J. Phys. B: Atom.Molec. Phys.***13** 3247

[131] Soloshenko I A, Tsiloko V V, Khomich V A, Bazhenov V Y, Ryabtsev A V, Schedrin A I and Mikhno I L 2002 *IEEE Trans. on Plasma Sci.***30** 1440-4

[132] Fehsenfeld F C, Mosesman M and Ferguson E E 1971 *J. Chem. Phys.***55** 2115-20

[133]Bierbaum V M, Golde M F and Kaufman F 1976 *J. Chem. Phys.***65** 2715-24

[134] Skalny J D, Orszagh J, Mason N J, Rees J A, Aranda-Gonzalvo Y and Whitmore T D 2008 *Int. J. Mass Spectrom.***272** 12-21

[135] Dunkin D B, Fehsenfeld F C and Ferguson E E 1970 *J. Chem. Phys.***53** 987-9

[136] McFarland M, Albritton D L, Fehsenfeld F C, Ferguson E E, Schmeltekopf A L 1973 *J. Chem. Phys.***59** 6629-35

[137] Fehsenfeld F C and Ferguson E E 1974 *J. Chem. Phys.***61** 3181-93

[138] Eichwald O, Yousfi M, Hennad A, Benabdessadok M D 1997 *J. Appl. Phys.***82** 4781

[139]Albritton D L 1978 *Atom.Data Nucl. Data Tables***22** 1-101

[140] Atkinson R, Baulch D L, Cox R A, Crowley J N, Hampson R F, Hynes R G, Jenkin M E, Rossi M J, Troe J 2006 http://www.iupac-kinetic.ch.cam.ac.uk.

[141] Atkinson R, Baulch D L, Cox R A, Hampson Jr. R F, Kerr J A, Rossi M J and Troe J 1997 *J. Phys. Chem. Ref. Data.***26** 1329-499

[142]Welge K H and Atkinson R 1976 *J. Chem. Phys.***64** 531

[143]Herron J T and Green D S 2001 *Plasma Chem. Plasma. Process.***21** 459-80

[144] Podolske J R and Johnston H S 1983 *J. Phys. Chem.***87** 628-34

[145] Palla A D, Carroll D L, Verdeyen J T and Solomon W C 2006 *J. Appl. Phys.***100** 023117

[146] Paul P H, Durant J L Jr, Gray J A, Furlanetto M R 1995 *J. Chem. Phys.***102** 8378-84

[147]Koike T and Morinaga K 1982 *Bull. Chem. Soc. Jpn.***55** 52-4

[148]*GRI-MECH 3 Reaction Rate Database*http://www.me.berkeley.edu/gri-mech/

[149] Mckendrick C B, Kerr E A and Wilkinson J P T 1984 *J. Phys. Chem.* **88** 3930-2

[150]Leblond J B, Collier F, Hoffbeck F and Cottin P 1981 *J. Chem.Phys.***74** 6242-55

[151]V. A. Godyak, Soviet Radio Frequency Discharge Research (Delphic Associates, Inc., Falls Church, VA, 1986).

[152]Sadeghi N, Setser D W and Touzeau M 2002 *J. Phys. Chem.* A **106** 8399-405

[153]Lichtenberg A J, Vahedi V, Lieberman M A and Rognlien T 1994*J. Appl. Phys.***75** 2339

[154] Novick S and Krenos J 1988 *J. Chem. Phys.***89** 7031-3

[155]Zhao G B, Argyle M D and Radosz M 2006*J. Appl. Phys.* **99** 113302

[156]Xiong Q, Nikiforov A Y, Lu1 X P and Leys C 2010 *J. Phys. D: Appl. Phys.***43** 415201

[157] Gudmundsson J T and Thorsteinsson E G 2007 *Plasma Sources Sci. Technol.***16** 399-412

[158] Itikawa Y, Ichimura A, Onda K, Sakimoto K, Takayanagi K, Hatano H, Hayashi M, Nishimura H, Tsurubuchi S 1989 *J. Phys. Chem. Ref. Data***18** 23-42

[159]Margreiter D, Deutsch H and Mark T D 1990 *Contrib. Plasma Phys.***30** 487

[160] Deng L, Shi W, Yang H, Sha G, Zhang C 2004 *Rev. Sci. Instruments***75** 4455-61

[161] Zipf E C 1969 *Canadian J. Chem.***47** 1863-70

[162] Binns W R and Ahl J L 1978 *J. Chem. Phys.***68** 538-46

[163] Neeser S, Kunz T and Langhoff J 1997 *J. Phys. D: Appl. Phys.***30** 1489

[164] Ashida S, Lee C and Lieberman M A 1995 *J. Vac. Sci.Technol.*A **13** 2498

[165]Skinner G B and Ringrose G H 1965 *J. Chem. Phys.***42** 2190-2

[166]Palla A D, Carroll D L, Verdeyen J T, Solomon W C 2006 *International Society for Optics and Photonics***6101** 610125-1

[167]Sheldon J W and Muschlitz E E Jr 1978 *J. Chern. Phys.***68** 5288

[168] Bourene M and Calve J L 1973 *J. Chern. Phys.***58** 1452

[169]*NIST chemical kinetic database*http://kinetics.nist.gov/kinetics/index.jsp

[170]Hadi-Ziane S, Held B and Pignolet P 1992 *J. Phys. D: Appl. Phys.***25** 677-85

[171]Stalder K R, Vidmar R J, Nersisyan G and Graham W G 2006 *J. Appl. Phys.***99** 093301

[172]Troe J 2011 *Combust. Flame***158** 594-601

[173]Kirkpatrick M, Dodet B and Odic E 2007 *Int. J. Plasma Environ. Sci. & Technol.* **1** 96-101